

# Early Neuron Alignment in Two-layer ReLU Networks with Small Initialization

Hancheng Min\*, René Vidal<sup>†</sup> and Enrique Mallada\*

\*Electrical and Computer Engineering, Johns Hopkins University

<sup>†</sup>Center for Innovation in Data Engineering and Science, University of Pennsylvania

July 25, 2023

## Abstract

This paper studies the problem of training a two-layer ReLU network for binary classification using gradient flow with small initialization. We consider a training dataset with well-separated input vectors: Any pair of input data with the same label are positively correlated, and any pair with different labels are negatively correlated. Our analysis shows that, during the early phase of training, neurons in the first layer try to align with either the positive data or the negative data, depending on its corresponding weight on the second layer. A careful analysis of the neurons' directional dynamics allows us to provide an  $\mathcal{O}(\frac{\log n}{\sqrt{\mu}})$  upper bound on the time it takes for all neurons to achieve good alignment with the input data, where  $n$  is the number of data points and  $\mu$  measures how well the data are separated. After the early alignment phase, the loss converges to zero at a  $\mathcal{O}(\frac{1}{t})$  rate, and the weight matrix on the first layer is approximately low-rank. Numerical experiments on the MNIST dataset illustrate our theoretical findings.

## 1 Introduction

Neural networks have shown excellent empirical performance in many application domains such as vision [1, 2], speech [3, 4] and video games [5, 6]. Despite being highly overparametrized, networks trained by gradient descent with random initialization and without explicit regularization enjoy good generalization performance. One possible explanation for this phenomenon is the implicit bias or regularization induced by first-order algorithms under certain initialization assumptions. For instance, first-order methods applied to (deep) matrix factorization models may produce solutions that have low nuclear norm [7] and/or low rank [8], and similar phenomena have been observed for deep tensor factorization [9]. Moreover, prior work such as [10, 11, 12, 13] has found that deep linear networks sequentially learn the dominant singular values of the input-output correlation matrix.

It is widely known that these sparsity-inducing biases can often be achieved by small initialization. This has motivated a series of works that theoretically analyze the training dynamics of first-order methods for neural networks with small initialization. For linear networks, the implicit bias of small initialization has been studied in the context of linear regression [10, 11, 14] and matrix factorization [7, 8, 15, 13, 12, 16]. Recently, the effect of small initialization has been studied for two-layer ReLU networks [17, 18, 19, 20]. For example, [17] observes that during the early stage of training, neurons in the first layer converge to one out of finitely many directions determined by the dataset. Based on this observation, [19] shows that in the case of well-separated data, where

any pair of input data with the same label are positively correlated and any pair with different labels are negatively correlated, there are only two directions the neurons tend to converge to: the positive data center and the negative one. Moreover, [19] shows that if such directional convergence holds, then the loss converges, and the resulting first-layer weight matrix is low-rank. However, directional convergence is assumed in their analysis; there is no explicit characterization of how long it takes to achieve directional convergence and how the time to convergence depends on the initialization scale.

## 1.1 Paper contributions

In this paper, we provide a complete analysis of the dynamics of gradient flow for the problem of training a two-layer ReLU network on well-separated data under the assumption of small initialization. Specifically, we show that if the initialization is sufficiently small, during the early phase of training the neurons in the first layer try to align with either the positive data or the negative data, depending on its corresponding weight on the second layer. Moreover, through a careful analysis of the neuron’s directional dynamics we show that the time it takes for all neurons to achieve good alignment with the input data is upper bounded by  $\mathcal{O}(\frac{\log n}{\sqrt{\mu}})$ , where  $n$  is the number of data points and  $\mu$  measures how well the data are separated. We also show that after the early alignment phase the loss converges to zero at a  $\mathcal{O}(\frac{1}{t})$  rate and that the weight matrix on the first layer is approximately low-rank.

**Notation:** We denote the Euclidean norm of a vector  $x$  by  $\|x\|$ , the inner product between vectors  $x$  and  $y$  by  $\langle x, y \rangle = x^\top y$ , and the cosine of the angle between them as  $\cos(x, y) = \langle \frac{x}{\|x\|}, \frac{y}{\|y\|} \rangle$ . For an  $n \times m$  matrix  $A$ , we let  $A^\top$  denote its transpose. We also let  $\|A\|_2$  and  $\|A\|_F$  denote the spectral norm and Frobenius norm of  $A$ , respectively. For a scalar-valued or matrix-valued function of time,  $F(t)$ , we let  $\dot{F} = \dot{F}(t) = \frac{d}{dt}F(t)$  denote its time derivative. Additionally, we define  $\mathbb{1}_A$  to be the indicator for a statement  $A$ :  $\mathbb{1}_A = 1$  if  $A$  is true and  $\mathbb{1}_A = 0$  otherwise. We also let  $I$  denote the identity matrix, and  $\mathcal{N}(\mu, \sigma^2)$  denote the normal distribution with mean  $\mu$  and variance  $\sigma^2$ .

## 2 Preliminaries

In this section, we first discuss the problem setting. We then present some key ingredients for analyzing the training dynamics of ReLU networks under small initialization, and discuss some of the weaknesses/issues from prior work.

### 2.1 Problem setting

We are interested in a binary classification problem with dataset  $[x_1, \dots, x_n] \in \mathbb{R}^{D \times n}$  (input data) and  $[y_1, \dots, y_n]^\top \in \{-1, +1\}^n$  (labels). For the classifier,  $f : \mathbb{R}^D \rightarrow \mathbb{R}$ , we consider a two-layer ReLU network:

$$f(x; W, v) = v^\top \sigma(W^\top x) = \sum_{j=1}^h v_j \sigma(w_j^\top x), \quad (1)$$

parametrized by network weights  $W := [w_1, \dots, w_h] \in \mathbb{R}^{D \times h}$ ,  $v := [v_1, \dots, v_h]^\top \in \mathbb{R}^{h \times 1}$ , where  $\sigma(\cdot) = \max\{\cdot, 0\}$  is the ReLU activation function. We aim to find the network weights that minimize the training loss  $\mathcal{L}(W, v) = \sum_{i=1}^n \ell(y_i, f(x_i; W, v))$ , where  $\ell : \mathbb{R} \times \mathbb{R} \rightarrow \mathbb{R}_{\geq 0}$  is the exponential loss  $\ell(y, \hat{y}) = \exp(-y\hat{y})$ . The network is trained via the gradient flow (GF) dynamics

$$\dot{W} \in \partial_W \mathcal{L}(W, v), \quad \dot{v} \in \partial_v \mathcal{L}(W, v), \quad (2)$$

where  $\partial_W \mathcal{L}, \partial_v \mathcal{L}$  are Clark sub-differentials of  $\mathcal{L}$ . Therefore, (2) is a differential inclusion [21]. The work of [20] shows that there exist global solutions to (2) if one uses  $\sigma'(x) = \mathbb{1}_{x>0}$  as the ReLU subgradient. Therefore, we follow this choice of subgradient for our analysis.

To initialize the weights, we consider the following initialization scheme. First, we start from a weight matrix  $W_0 \in \mathbb{R}^{D \times h}$ , and then and then initialize the weights as

$$W(0) = \epsilon W_0, \quad v_j(0) \in \{\|w_j(0)\|, -\|w_j(0)\|\}, \forall j \in [h]. \quad (3)$$

That is, the weight matrix  $W_0$  determines the initial shape of the first-layer weights  $W(0)$  and we use  $\epsilon$  to control the initialization scale and we are interested in the regime where  $\epsilon$  is sufficiently small. For the second layer weights  $v(0)$ , each  $v_j(0)$  has magnitude  $\|w_j(0)\|$  and we only need to decide its sign. Our results in later sections are stated for a deterministic choice of  $\epsilon, W_0$ , and  $v(0)$ , then we comment on the case where  $W_0$  is chosen randomly via some distribution.

The resulting weights in (3) are always "balanced", i.e.,  $v_j^2(0) - \|w_j(0)\|^2 = 0, \forall j \in [h]$ , because  $v_j(0)$  can only take two values: either  $\|w_j(0)\|$  or  $-\|w_j(0)\|$ . More importantly, under GF (2), this balancedness is preserved [22]:  $v_j^2(t) - \|w_j(t)\|^2 = 0, \forall t \geq 0, \forall j \in [h]$ . In addition, it is shown in [20] that  $\text{sign}(v_j(t)) = \text{sign}(v_j(0)), \forall t \geq 0, \forall j \in [h]$ , and the dynamical behaviors of neurons will be divided into two types, depending on  $\text{sign}(v_j(0))$ .

**Remark 1.** *For our theoretical results, the balancedness condition is assumed for technical purposes: it simplifies the dynamics of GF and thus the analysis. It is a common assumption for many existing works on both linear [23] and nonlinear [19, 20] neural networks. For the experiments in Section 4, we use a standard Gaussian initialization with small variance, which is not balanced.*

**Remark 2.** *Without loss of generality, we consider the case where all columns of  $W_0$  are nonzero, i.e.,  $\|w_j(0)\| > 0, \forall j \in [h]$ . We make this assumption because whenever  $w_j(0) = 0$ , we also have  $v_j(0) = 0$  from the balancedness, which together would imply  $\dot{v}_j \equiv 0, \dot{w}_j \equiv 0$  under gradient flow. As a result,  $w_j$  and  $v_j$  would remain zero and thus they could be ignored in the convergence analysis.*

**Remark 3.** *Our main results will depend on both  $\max_j \|w_j(0)\|$  and  $\min_j \|w_j(0)\|$ , as shown in our proofs in Appendices C and D. Therefore, whenever we speak of small initialization, we will say that  $\epsilon$  is small without worrying about the scale of  $W_0$ , which is already considered in our results.*

## 2.2 Neural alignment with small initialization: an overview

Prior work argues that the gradient flow dynamics (2) under small initialization (3), i.e., when  $\epsilon$  is sufficiently small, can be roughly described as "align then fit" [17, 20] (We also refer readers to Appendix B for a detailed explanation with dynamical equations for  $\|w_j\|$  and  $\frac{w_j}{\|w_j\|}$ ): During the early phase of training, every neuron  $w_j, j \in [h]$  keeps a small norm  $\|w_j\|^2 \ll 1$  while changing their directions  $\frac{w_j}{\|w_j\|}$  significantly in order to locally maximize a "signed coverage" [17] of itself w.r.t. the training data. After the alignment phase, part of the neurons (potentially all neurons) start to grow their norms in order to fit the training data, and the loss decreases significantly. The analysis for the fitting phase generally depends on the resulting neuron directions at the end of the alignment phase [19, 20]. However, prior analysis of the alignment phase either is based on a vanishing initialization argument that can not be directly translated into the case finite but small initialization [17] or assumes some stringent assumption on the data [20]. In this section, we provide a brief overview of the existing analysis for neural alignment and then point out several weaknesses in prior work.

**Prior analysis of the alignment phase:** Since during the alignment phase all neurons have small norm, prior work mainly focuses on the directional dynamics, i.e.,  $\frac{d}{dt} \frac{w_j}{\|w_j\|}$ , of the neurons. The analysis relies on the following approximation of the dynamics of every neuron  $w_j, j \in [h]$ :

$$\frac{d}{dt} \frac{w_j}{\|w_j\|} \simeq \text{sign}(v_j(0)) \mathcal{P}_{w_j} x_a(w_j), \quad (4)$$

where  $\mathcal{P}_w = I - \frac{ww^\top}{\|w\|^2}$  is the projection onto the subspace orthogonal to  $w$  and

$$x_a(w) := \sum_{i: \langle x_i, w \rangle > 0} y_i x_i \quad (5)$$

denotes the signed combination of the data points activated by  $w$ . First of all, (4) implies that the dynamics  $\frac{w_j}{\|w_j\|}$  are approximately decoupled, and thus one can study each  $\frac{w_j}{\|w_j\|}$  separately. Moreover, as illustrated in Figure 1, if  $\text{sign}(v_j(0)) > 0$ , the flow (4) pushes  $w_j$  towards  $x_a(w_j)$ , since  $w_j$  is attracted by its currently activated positive data and repelled by its currently activated negative data. Intuitively, during the alignment phase, a neuron  $w_j$  with  $\text{sign}(v_j(0)) > 0$  would try to find a direction where it can activate as much positive data and as less negative data as possible. If  $\text{sign}(v_j(0)) < 0$ , the opposite holds.

Indeed, [17] claims that the neuron  $w_j$  would be aligned with some "extreme vectors," defined as vector  $w \in S^{D-1}$  that locally maximizes  $\sum_{i \in [n]} y_i \sigma(\langle x_i, w \rangle)$  (similarly,  $w_j$  with  $\text{sign}(v_j(0)) < 0$  would be aligned with the local minimizer), and there are only finitely many such vectors; thus the neurons are expected to converge to one of these extreme vectors in direction. The analysis is done by taking the limit  $\epsilon \rightarrow 0$  on the initialization scale, under which the approximation in (4) is exact.

**Weakness in prior analyses:** Although [17] provides great insights into the dynamical behavior of the neurons in the alignment phase, the validity of the aforementioned approximation for finite but small  $\epsilon$  remains in question. First, one needs to make sure that the error  $\left\| \frac{d}{dt} \frac{w_j}{\|w_j\|} - \text{sign}(v_j(0)) \mathcal{P}_{w_j} x_a(w_j) \right\|$  is sufficiently small when  $\epsilon$  is finite in order to justify (4) as a good approximation. Second, the error bound needs to hold for the entire alignment phase. [17] assumes  $\epsilon \rightarrow 0$ ; hence there is no formal error bound. In addition, prior analyses on small initialization [12, 20] suggest the alignment phase only holds for  $\Theta(\log \frac{1}{\epsilon})$  time. Thus, the claim in [17] would only hold if good alignment is achieved before the alignment phase ends. However, [17] provides no upper bound on the time it takes to achieve good alignment. Therefore, without a finite  $\epsilon$  analysis, [17] fails to fully explain the training dynamics under small initialization. Understanding the alignment phase with finite  $\epsilon$  requires additional analytical tools from dynamical systems theory. To the best of our knowledge, this has only been studied under a stringent assumption that all data points are orthogonal to each other [20].

**Goal of this paper:** In this paper, we want to address some of the aforementioned issues by developing a formal analysis for the early alignment phase with a finite but small initialization scale  $\epsilon$ . We first discuss our main theorem that shows that a directional convergence can be achieved within bounded time under data assumptions that are less restrictive and have more practical relevance. Then, we discuss the error bound for justifying (4) in the proof sketch for the main theorem.

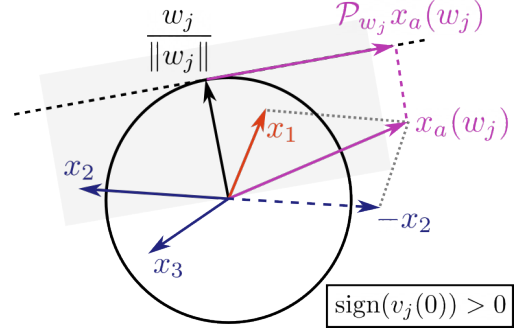


Figure 1: Illustration of  $\frac{d}{dt} \frac{w_j}{\|w_j\|}$  during the early alignment phase.  $x_1$  has +1 label, and  $x_2, x_3$  have -1 labels,  $x_1, x_2$  lie inside the halfspace  $\langle x, w_j \rangle > 0$  (gray shaded), thus  $x_a(w_j) = x_1 - x_2$ . Since  $\text{sign}(v_j(0)) > 0$ , GF pushes  $w_j$  towards  $x_a(w_j)$ .

### 3 Convergence of Two-layer ReLU Networks with Small Initialization

In this section, we present our main results, which require the following assumption on the training data (we will compare our assumption with those in prior work after the main theorem):

**Assumption 1.** Any pair of input data with the same label are positively correlated, and any pair of inputs with different labels are negatively correlated, i.e.,

$$\min_{i,j} \frac{\langle x_i y_i, x_j y_j \rangle}{\|x_i\| \|x_j\|} := \mu > 0. \quad (6)$$

Given a training dataset, we define  $\mathcal{S}_+ := \{z \in \mathbb{R}^D : \mathbb{1}_{\langle x_i, z \rangle > 0} = \mathbb{1}_{y_i > 0}, \forall i\}$  to be the cone in  $\mathbb{R}^n$  such that whenever neuron  $w \in \mathcal{S}_+$ ,  $w$  is activated exclusively by every  $x_i$  with a positive label (see Figure 2). Similarly, for  $x_i$  with negative labels, we define  $\mathcal{S}_- := \{z \in \mathbb{R}^D : \mathbb{1}_{\langle x_i, z \rangle > 0} = \mathbb{1}_{y_i < 0}, \forall i\}$ . Finally, we define  $\mathcal{S}_{\text{dead}} := \{z \in \mathbb{R}^D : \langle z, x_i \rangle \leq 0, \forall i\}$  to be the cone such that whenever  $w \in \mathcal{S}_{\text{dead}}$ , no data activates  $w$ . Given Assumption 1, it can be shown (see Appendix C) that  $\mathcal{S}_+$  ( $\mathcal{S}_-$ ) is a non-empty, convex cone that contains all positive data  $x_i, i \in \mathcal{I}_+$  (negative data  $x_i, i \in \mathcal{I}_-$ ).  $\mathcal{S}_{\text{dead}}$  is a convex cone as well, but not necessarily non-empty. We illustrate these cones in Figure 2 given some training data (red solid arrow denotes positive data and blue denotes negative ones).

Moreover, given some initialization from (3), we define  $\mathcal{I}_+ := \{i \in [n] : y_i > 0\}$  to be the set of indices of positive data, and  $\mathcal{I}_- := \{i \in [n] : y_i < 0\}$  for negative data. We also define  $\mathcal{V}_+ := \{j \in [h] : \text{sign}(v_j(t)) > 0\}$  to be the set of indices of neurons with positive second-layer entry and  $\mathcal{V}_- := \{j \in [h] : \text{sign}(v_j(t)) < 0\}$  for neurons with negative second-layer entry. Note that, as discussed in Section 2.1,  $\text{sign}(v_j(t))$  does not change under balanced initialization, thus  $\mathcal{V}_+, \mathcal{V}_-$  are time invariant. Further, as we discussed in Section 2.2 about the early alignment phase, we expect that every neuron in  $\mathcal{V}_+$  will drift toward the region where positive data concentrate and thus eventually reach  $\mathcal{S}_+$  or  $\mathcal{S}_{\text{dead}}$ , as visualized in Figure 2 ( $x_+, x_-$  shown in the figure are defined in Assumption 2). Similarly, all neurons in  $\mathcal{V}_-$  would chase after negative data and thus reach  $\mathcal{S}_-$  or  $\mathcal{S}_{\text{dead}}$ . Our theorem precisely characterizes this behavior.

#### 3.1 Main results

Before we present our main theorem, we need the following assumption on the initialization, mostly for technical reasons.

**Assumption 2.** The initialization from (3) satisfies that  $\max_{j \in \mathcal{V}_+} \langle \frac{w_j(0)}{\|w_j(0)\|}, \frac{x_-}{\|x_-\|} \rangle < 1$ , and  $\max_{j \in \mathcal{V}_-} \langle \frac{w_j(0)}{\|w_j(0)\|}, \frac{x_+}{\|x_+\|} \rangle < 1$ , where  $x_+ = \sum_{i \in \mathcal{I}_+} x_i$  and  $x_- = \sum_{i \in \mathcal{I}_-} x_i$ .

Assumption (2) essentially asks the neuron  $w_j(0), j \in \mathcal{V}_+$  (or  $w_j(0), j \in \mathcal{V}_-$ , resp.) to not be completely aligned with  $x_+$  (or  $x_-$ , resp.).

We are now ready to present our main result (given Assumption 1 and Assumption 2):

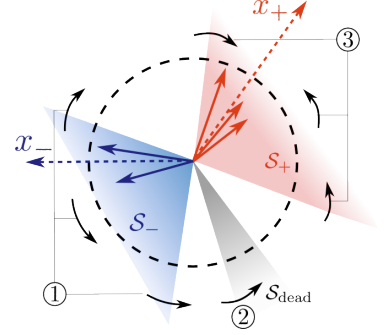


Figure 2: Neuron alignment under data that satisfies Assumption 1. For neurons in  $\mathcal{V}_+$ , ① if it lies inside  $\mathcal{S}_-$ , then it gets repelled by  $x_-$  and eventually escapes  $\mathcal{S}_-$ ; Once it is outside  $\mathcal{S}_-$ , it may ② get continuously repelled by some negative data and eventually enters  $\mathcal{S}_{\text{dead}}$ . or ③ gain some activation on positive data and eventually enter  $\mathcal{S}_+$ , after which it gets constantly attracted by  $x_+$ .

**Theorem 1.** *Given some initialization from (3), if  $\epsilon = \mathcal{O}(\frac{1}{\sqrt{h}} \exp(-\frac{n}{\sqrt{\mu}} \log n))$ , then any solution to the gradient flow dynamics (2) satisfies*

1. (Directional convergence in early alignment phase)  $\exists t_1 = \mathcal{O}(\frac{\log n}{\sqrt{\mu}})$ , such that
  - $\forall j \in \mathcal{V}_+$ , either  $w_j(t_1) \in \mathcal{S}_+$  or  $w_j(t_1) \in \mathcal{S}_{dead}$ . Moreover, if  $\max_{i \in \mathcal{I}_+} \langle w_j(0), x_i \rangle > 0$ , then  $w_j(t_1) \in \mathcal{S}_+$ .
  - $\forall j \in \mathcal{V}_-$ , either  $w_j(t_1) \in \mathcal{S}_-$  or  $w_j(t_1) \in \mathcal{S}_{dead}$ . Moreover, if  $\max_{i \in \mathcal{I}_-} \langle w_j(0), x_i \rangle > 0$ , then  $w_j(t_1) \in \mathcal{S}_-$ .
2. (Final convergence and low-rank bias)  $\forall t \geq t_1$  and  $\forall j \in [h]$ , neuron  $w_j(t)$  stays within  $\mathcal{S}_+$  ( $\mathcal{S}_-$ , or  $\mathcal{S}_{dead}$ ) if  $w_j(t_1) \in \mathcal{S}_+$  ( $\mathcal{S}_-$ , or  $\mathcal{S}_{dead}$  resp.). Moreover, if both  $\mathcal{S}_+$  and  $\mathcal{S}_-$  contains at least one neuron at time  $t_1$ , then
  - $\exists \alpha > 0$  and  $\exists t_2$  with  $t_1 \leq t_2 = \Theta(\frac{1}{n} \log \frac{1}{\sqrt{h\epsilon}})$ , such that  $\mathcal{L}(t) \leq \frac{\mathcal{L}(t_2)}{\mathcal{L}(t_2)^\alpha (t-t_2)+1}$ ,  $\forall t \geq t_2$ .
  - As  $t \rightarrow \infty$ ,  $\|W(t)\| \rightarrow \infty$  and  $\|W(t)\|_F^2 \leq 2\|W(t)\|_2^2 + \mathcal{O}(\epsilon)$ . Thus, the stable rank of  $W(t)$  satisfies  $\limsup_{t \rightarrow \infty} \|W(t)\|_F^2 / \|W(t)\|_2^2 \leq 2$ .

We provide a proof sketch that highlights the technical novelty of our results in Section 3.2. Our  $\mathcal{O}(\cdot)$  notations hide additional constants that depend on the data and initialization, for which we refer readers to the complete proof of Theorem 1 in Appendix C and D. We make the following remarks:

**Early neuron alignment:** The first part of the Theorem 1 describes the configuration of *all* neurons at the end of the alignment phase. Every neuron in  $\mathcal{V}_+$  reaches either  $\mathcal{S}_+$  or  $\mathcal{S}_{dead}$  by  $t_1$ , and stays there for the remainder of training. Obviously, we care about those neurons reaching  $\mathcal{S}_+$  as any neuron in  $\mathcal{S}_{dead}$  does not contribute to the final convergence at all. Luckily, Theorem 1 suggests that any neuron in  $\mathcal{V}_+$  that starts with some activation on the positive data, i.e., it is initialized in the union of halfspaces  $\cup_{i \in \mathcal{I}_+} \{w : \langle w, x_i \rangle > 0\}$ , will eventually reach  $\mathcal{S}_+$ . A similar discussion holds for neurons in  $\mathcal{V}_-$ . We argue that randomly initializing  $W_0$  ensures that with high probability, there will be at least a pair of neurons reaching  $\mathcal{S}_+$  and  $\mathcal{S}_-$  by time  $t_1$  (please see the next remark). Lastly, we note that it is possible that  $\mathcal{S}_{dead} = \emptyset$ , in which case every neuron reaches either  $\mathcal{S}_+$  or  $\mathcal{S}_-$ .

**Merits of random initialization:** Our theorem is stated for a deterministic initialization (3) given an initial shape  $W_0$ . In practice, one would use random initialization to find a  $W_0$ , for example,  $[W_0]_{ij} \stackrel{i.i.d.}{\sim} \mathcal{N}(0, 1/D)$ . First, our Theorem 1 applies to this Gaussian initialization: Assumption 2 is satisfied with probability one because the events  $\langle \frac{w_j(0)}{\|w_j(0)\|}, \frac{x_-}{\|x_-\|} \rangle = 1$  and  $\langle \frac{w_j(0)}{\|w_j(0)\|}, \frac{x_+}{\|x_+\|} \rangle = 1$  have probability zero. Moreover, any neuron in  $\mathcal{V}_+$  has at least probability 1/2 of being initialized within the union of halfspaces  $\cup_{i \in \mathcal{I}_+} \{w : \langle w, x_i \rangle > 0\}$ , which ensures that this neuron reaches  $\mathcal{S}_+$ . Thus when there are  $m$  neurons in  $\mathcal{V}_+$ , the probability that  $\mathcal{S}_+$  has at least one neuron at time  $t_1$  is lower bounded by  $1 - 2^{-m}$  (same argument holds for  $\mathcal{S}_-$ ), Therefore, with only very mild overparametrization on the network width  $h$ , one can make sure that with high probability there is at least one neuron in both  $\mathcal{S}_+$  and  $\mathcal{S}_-$ , leading to final convergence.

**Duration of alignment phase:** Our theorem shows that for sufficiently small  $\epsilon$ , directional convergence, i.e., all neurons reaching either  $\mathcal{S}_+$ ,  $\mathcal{S}_-$ ,  $\mathcal{S}_{dead}$ , is achieved within  $\mathcal{O}(\frac{\log n}{\sqrt{\mu}})$  time (notably, independent of  $\epsilon$ ). Our bound quantitatively reveals the non-trivial dependency on the "data separation"  $\mu$  for such directional convergence to occur. To the best of our knowledge, this is the first non-asymptotic bound on the time it takes for all neurons to achieve a desired configuration. [17] only shows such  $t_1 > 0$  exists using an  $\epsilon \rightarrow 0$  argument, without analyzing how large  $t_1$  can be. [20] studies a different data assumption (we compare it with ours in later remarks) under which the

alignment is studied only for neurons that has a specific activation pattern at initialization. Lastly, we note that  $\mu \rightarrow 0$  leads to  $t_1 \rightarrow \infty$ , this is because when  $\mu = 0$ , there are more limiting directions to which neurons can converge, hence not all of them are "attracted" by  $\mathcal{S}_+$ ,  $\mathcal{S}_-$ ,  $\mathcal{S}_{\text{dead}}$ .

**Refined alignment within  $\mathcal{S}_+$ ,  $\mathcal{S}_-$ :** Once a neuron in  $\mathcal{V}_+$  reaches  $\mathcal{S}_+$ , it never leaves  $\mathcal{S}_+$ . Moreover, it always gets attracted by  $x_+$ . Therefore, every neuron gets well aligned with  $x_+$ , i.e.,  $\cos(w_j, x_+) \simeq 1, \forall w_j \in \mathcal{S}_+$ . A similar argument shows neurons in  $\mathcal{S}_-$  get attracted by  $x_-$ . We opt not to formally state it in Theorem 1 as the result would be similar to that in [20], and alignment with  $x_+, x_-$  is not necessary to guarantee convergence. Instead, we show this refined alignment through our numerical experiment in Section 4.

**Final convergence and low-rank bias:** The convergence analysis after  $t_1$  is simple: All neurons in  $\mathcal{S}_{\text{dead}}$  have small norm and do not move thus they can be ignored from the analysis. More interestingly, GF after  $t_1$  can be viewed as fitting positive data  $x_i, i \in \mathcal{I}_+$ , with a subnetwork consisting of all neurons in  $\mathcal{S}_+$ , and fitting negative data with neurons in  $\mathcal{S}_-$ . By the fact that all neurons in  $\mathcal{S}_+$  activate all  $x_i, i \in \mathcal{I}_+$ , the resulting subnetwork is linear, and so is the subnetwork for fitting  $x_i, i \in \mathcal{I}_-$ . The convergence analysis reduces to establishing  $\mathcal{O}(1/t)$  convergence for two linear networks [24, 14, 25]. As for the stable rank, our result follows the analysis in [26], but in a simpler form since ours is for linear networks.

**Comparison with [19]:** Prior work [19] considers a similar data assumption to ours. However, [19] assumes that there exists a time  $t_1$  such that at  $t_1$ , the neurons are in either  $\mathcal{S}_+$ ,  $\mathcal{S}_-$  or  $\mathcal{S}_{\text{dead}}$  and their main contribution is the analysis of the implicit bias for the later stage of the training. [19] justifies their assumption by the analysis in [17], which does not necessarily apply to the case of finite  $\epsilon$ , as we discussed in Section 2.2. Our work precisely establishes such directional convergence for finite but small  $\epsilon$ , showing indeed the neurons achieve some good alignment with  $x_+, x_-$  within  $\mathcal{O}(\frac{\log n}{\sqrt{\mu}})$  time before they start to grow in norm. Moreover, [19] has no characterization on the convergence rate of the loss after the alignment phase, while we provide a  $\mathcal{O}(1/t)$  bound on the loss. In addition, [19] considers the case where input data  $x_i, i \in [n]$ , spans the entire  $\mathbb{R}^D$ , which leads to  $\mathcal{S}_{\text{dead}} = \emptyset$ . This implicitly imposes the constraint that the number of data points  $n$  must be larger than the input dimension  $D$ . Our analysis allows for the case  $\mathcal{S}_{\text{dead}} \neq \emptyset$  as we provide a sufficient condition for preventing a neuron from reaching  $\mathcal{S}_{\text{dead}}$ .

**Comparison with [20]:** In [20], the neuron alignment is carefully analyzed for the case all data points are orthogonal to each other, i.e.,  $\langle x_i, x_j \rangle = 0, \forall i \neq j \in [n]$ . Such an assumption restricts the number of data points  $n$  to be smaller than the input dimension  $D$  and is often unrealistic. Our assumption does not restrict the size of the dataset and thus has more practical relevance (see our numerical experiments in Section 4).

### 3.2 Proof sketch for the alignment phase

In this section, we sketch the proof for our Theorem 1. First of all, it can be shown that  $\mathcal{S}_+, \mathcal{S}_{\text{dead}}$  are trapping regions for all  $w_j(t), j \in \mathcal{V}_+$ , that is, whenever  $w_j(t)$  gets inside  $\mathcal{S}_+$  (or  $\mathcal{S}_{\text{dead}}$ ), it never leaves  $\mathcal{S}_+$  (or  $\mathcal{S}_{\text{dead}}$ ). Similarly,  $\mathcal{S}_-, \mathcal{S}_{\text{dead}}$  are trapping regions for all  $w_j(t), j \in \mathcal{V}_-$ . The alignment phase analysis concerns how long it takes for all neurons to reach one of the trapping regions, followed by the final convergence analysis on fitting data with +1 label by neurons in  $\mathcal{S}_+$  and fitting data with -1 label by those in  $\mathcal{S}_-$ . We have discussed the final convergence analysis in the remark "Final convergence and low-rank bias", thus we focus on the proof sketch for the early alignment phase here, which is considered as our main technical contribution.

**Approximating  $\frac{d}{dt} \frac{w_j}{\|w_j\|}$ :** Our analysis for the neural alignment is rooted in the following Lemma:

**Lemma 1.** Given some initialization from (3), if  $\epsilon = \mathcal{O}(\frac{1}{\sqrt{h}})$ , then there exists  $T = \Theta(\frac{1}{n} \log \frac{1}{\sqrt{h\epsilon}})$  such that any solution to the gradient flow dynamics (2) satisfies that  $\forall t \leq T$ ,

$$\max_j \left\| \frac{d}{dt} \frac{w_j(t)}{\|w_j(t)\|} - \text{sign}(v_j(0)) \mathcal{P}_{w_j(t)} x_a(w_j(t)) \right\| = \mathcal{O}(\epsilon n \sqrt{h}). \quad (7)$$

This Lemma shows that the error between  $\frac{d}{dt} \frac{w_j(t)}{\|w_j(t)\|}$  and  $\text{sign}(v_j(0)) \mathcal{P}_{w_j(t)} x_a(w_j(t))$  can be arbitrarily small with some appropriate choice of  $\epsilon$  (to be determined later). This allows one to analyze the true directional dynamics  $\frac{w_j(t)}{\|w_j(t)\|}$  using some property of  $\mathcal{P}_{w_j(t)} x_a(w_j(t))$ , which leads to a  $t_1 = \mathcal{O}(\frac{\log n}{\sqrt{\mu}})$  upper bound on the time it takes for the neuron direction to converge to the sets  $\mathcal{S}_+$ ,  $\mathcal{S}_-$ , or  $\mathcal{S}_{\text{dead}}$ . Moreover, it also suggests  $\epsilon$  can be made sufficiently small so that the error bound holds until the directional convergence is achieved, i.e.  $T \geq t_1$ . We will first illustrate the analysis for directional convergence, then close the proof sketch with the choice of a sufficiently small  $\epsilon$ .

**Activation pattern evolution:** Given a sufficiently small  $\epsilon$ , one can show that under Assumption 1, for every neuron  $w_j$  that is not in  $\mathcal{S}_{\text{dead}}$  we have:

$$\frac{d}{dt} \left\langle \frac{w_j}{\|w_j\|}, \frac{x_i y_i}{\|x_i\|} \right\rangle \Big|_{\langle w_i, x_i \rangle = 0} > 0, \forall i \in [n], \text{ if } j \in \mathcal{V}_+, \quad (8)$$

$$\frac{d}{dt} \left\langle \frac{w_j}{\|w_j\|}, \frac{x_i y_i}{\|x_i\|} \right\rangle \Big|_{\langle w_i, x_i \rangle = 0} < 0, \forall i \in [n], \text{ if } j \in \mathcal{V}_-. \quad (9)$$

This is because whenever a neuron satisfies  $\langle x_i, w_j \rangle = 0$  for some  $i$ , and has activation on some other data, GF moves  $w_j$  towards  $x_a(w_j) = \sum_{i: \langle x_i, w_j \rangle > 0} x_i y_i$ . Interestingly, Assumption 1 implies  $\langle x_i y_i, x_a(w_j) \rangle > 0, \forall i \in [n]$ , which makes  $\frac{d}{dt} \frac{w_j}{\|w_j\|} \simeq \text{sign}(v_j(0)) \mathcal{P}_{w_j} x_a(w_j)$  point inward (or outward) the halfspace  $\langle x_i y_i, w_j \rangle > 0$ , if  $\text{sign}(v_j(0)) > 0$  (or  $\text{sign}(v_j(0)) < 0$ , respectively). See Figure 3 for illustration.

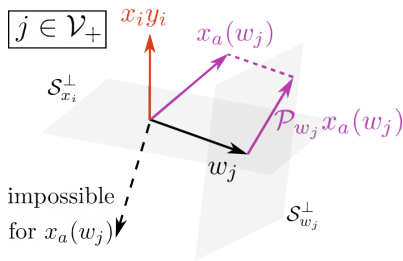


Figure 3: For  $j \in \mathcal{V}_+$ , Assumption 1 enforces  $\langle x_i y_i, x_a(w_j) \rangle > 0$ , thus GF pushes  $w_j$  inward the halfspace  $\langle x_i y_i, w_j \rangle > 0$  at  $\langle x_i, w_j \rangle = 0$  (i.e. towards gaining activation on  $x_i$ , if  $y_i = +1$ , or losing activation on  $x_i$ , if  $y_i = -1$ ).  $\mathcal{S}_{x_i}^\perp$  and  $\mathcal{S}_{w_j}^\perp$  denotes the subspace orthogonal to  $x_i$  and  $w_j$ , respectively.

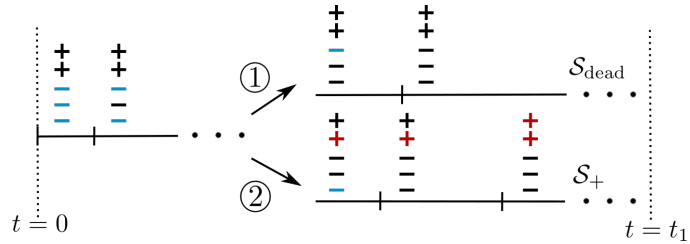


Figure 4: Illustration of the activation pattern evolution. The epochs on the time axis denote the time  $w_j$  changes its activation pattern by either losing one negative data (denoted by "+") or gaining one positive data (denoted by "-"). The markers are colored if it currently activates  $w_j$ . During the alignment phase  $0 \leq t \leq t_1$ , a neuron  $w_j, j \in \mathcal{V}_+$  starts with activation on all negative data and no positive data, every  $\mathcal{O}(1/n_a)$  time, it must change its activation, unless either ① it reaches  $\mathcal{S}_{\text{dead}}$ , or ② it activates some positive data at some epoch then eventually reaches  $\mathcal{S}_+$ .

As a consequence, a neuron can only change its activation pattern in a particular manner: a neuron in  $\mathcal{V}_+$ , whenever it is activated by some  $x_i$  with  $y_i = +1$ , never loses the activation on



$x_i$  thereafter, because (8) implies that GF pushes  $\frac{w_j}{\|w_j\|}$  towards  $x_i$  at the boundary  $\langle w_j, x_i \rangle = 0$ . Moreover, (8) also shows that a neuron in  $\mathcal{V}_+$  will never regain activation on a  $x_i$  with  $y_i = -1$  once it loses the activation because GF pushes  $\frac{w_j}{\|w_j\|}$  against  $x_i$  at the boundary  $\langle w_i, x_i \rangle = 0$ . Similarly, a neuron in  $\mathcal{V}_-$  never loses activation on negative data and never gains activation on positive data.

**Bound on activation transitions and duration:** Equations (8) and (9) are key in the analysis of alignment because they limit how many times a neuron can change its activation pattern: a neuron in  $\mathcal{V}_+$  can only gain activation on positive data and lose activation on negative data, thus at maximum, a neuron  $w_j$ ,  $j \in \mathcal{V}_+$ , can start with full activation on all negative data and no activation on any positive one (which implies  $w_j(0) \in \mathcal{S}_-$ ) then lose activation on every negative data and gain activation on every positive data as GF training proceeds (which implies  $w_j(t_1) \in \mathcal{S}_+$ ), taking at most  $n$  changes on its activation pattern. See Figure 4 for an illustration. Then, since it is possible to show that a neuron  $w_j$  with  $j \in \mathcal{V}_+$  that has  $\cos(w_j, x_-) < 1$  (guaranteed by Assumption 2) and is not in  $\mathcal{S}_+$  or  $\mathcal{S}_{\text{dead}}$ , must change its activation pattern after  $\mathcal{O}(\frac{1}{n_a \sqrt{\mu}})$  time (that does not depend on  $\epsilon$ ), where  $n_a$  is the number of data that currently activates  $w_j$ , one can upper bound the time for  $w_j$  to reach  $\mathcal{S}_+$  or  $\mathcal{S}_{\text{dead}}$  by some  $t_1 = \mathcal{O}(\frac{\log n}{\sqrt{\mu}})$  constant independent of  $\epsilon$ . Moreover,  $w_j$  must reach  $\mathcal{S}_+$  if it initially has activation on at least one positive data, i.e.,  $\max_{i \in \mathcal{I}_+} \langle w_j(0), x_i \rangle > 0$  since it cannot lose this activation. A similar argument holds for  $w_j, j \in \mathcal{V}_-$  that they reaches either  $\mathcal{S}_-$  or  $\mathcal{S}_{\text{dead}}$  before  $t_1$ .

**Choice of  $\epsilon$ :** All the aforementioned analyses rely on the assumption that the approximation in equation (4) holds with some specific error bound. We show in Appendix C that the desired bound is  $\left\| \frac{d}{dt} \frac{w_j(t)}{\|w_j(t)\|} - \text{sign}(v_j(0)) \mathcal{P}_{w_j(t)} x_a(w_j(t)) \right\| \leq \mathcal{O}(\sqrt{\mu})$ , which, by Lemma 1, can be achieved by a sufficiently small initialization scale  $\epsilon_1 = \mathcal{O}(\frac{\sqrt{\mu}}{\sqrt{hn}})$ . Moreover, the directional convergence (which takes  $\mathcal{O}(\frac{\log n}{\sqrt{\mu}})$  time) should be achieved before the alignment phase ends, which happens at  $T = \Theta(\frac{1}{n} \log \frac{1}{\sqrt{h\epsilon}})$ . This is ensured by choosing another sufficiently small initialization scale  $\epsilon_2 = \mathcal{O}(\frac{1}{\sqrt{h}} \exp(-\frac{n}{\sqrt{\mu}} \log n))$ . Overall, the initialization scale should satisfy  $\epsilon \leq \min\{\epsilon_1, \epsilon_2\}$ . We opt to present  $\epsilon_2$  in our main theorem because  $\epsilon_2$  beats  $\epsilon_1$  when  $n$  is large.

## 4 Numerical Experiments

### 4.1 Illustrative example

We first illustrate our theorem using a toy example: we train a two-layer ReLU network with  $h = 50$  neurons under a toy dataset in  $\mathbb{R}^2$  (See Figure. 5) that satisfies our Assumption 1, and initialize all entries of the weights as  $[W]_{ij} \stackrel{i.i.d.}{\sim} \mathcal{N}(0, \alpha)$ ,  $v_j \stackrel{i.i.d.}{\sim} \mathcal{N}(0, \alpha)$ ,  $\forall i \in [n], j \in [h]$  with  $\alpha = 10^{-6}$ . Then we run gradient descent on both  $W$  and  $v$  with step size  $\eta = 2 \times 10^{-3}$ . Our theorem well predicts the dynamics of neurons at the early stage of the training: aside from neurons that ended up in  $\mathcal{S}_{\text{dead}}$ , neurons in  $\mathcal{V}_+$  reach  $\mathcal{S}_+$  and achieve good alignment with  $x_+$ , and neurons in  $\mathcal{V}_-$  are well aligned with  $x_-$  in  $\mathcal{S}_-$ . Note that after alignment, the loss experiences two sharp decreases before it gets close to zero, which is studied and explained in [20].

### 4.2 Binary classification on two MNIST digits

Next, we consider a binary classification task for two MNIST digits. Such training data do not satisfy Assumption 1 since every data vector is a grayscale image with non-negative entries, making the inner product between any pair of data non-negative, regardless of their labels. However, we

can preprocess the training data by centering:  $x_i \leftarrow x_i - \bar{x}$ , where  $\bar{x} = \sum_{i \in [n]} x_i / n$ . The preprocessed data, then, approximately satisfies our assumption (see the left-most plot in Figure 6): a pair of data points is very likely to have a positive correlation if they have the same label and to have a negative correlation if they have different labels. Thus we expect our theorem to make reasonable predictions on the training dynamics with preprocessed data. For the remaining part of this section,

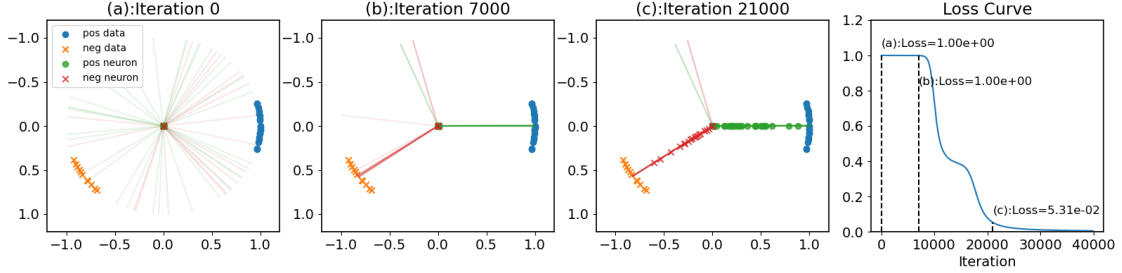


Figure 5: Illustration of gradient descent on two-layer ReLU network with small initialization. The marker represents either a data point or a neuron. Solid lines represent the directions of neurons. (a) at initialization, all neurons have small norm and are pointing in different directions; (b) around the end of the alignment phase, all neurons are in  $\mathcal{S}_+$ ,  $\mathcal{S}_-$ , or  $\mathcal{S}_{\text{dead}}$ . Moreover, neurons in  $\mathcal{S}_+$  ( $\mathcal{S}_-$ ) are well aligned with  $x_+$  ( $x_-$ ); (c) With good alignment, neurons in  $\mathcal{S}_-$ ,  $\mathcal{S}_+$  start to grow in norm and the loss decreases. When the loss is close to zero, the resulting network has its first-layer weight approximately low-rank.

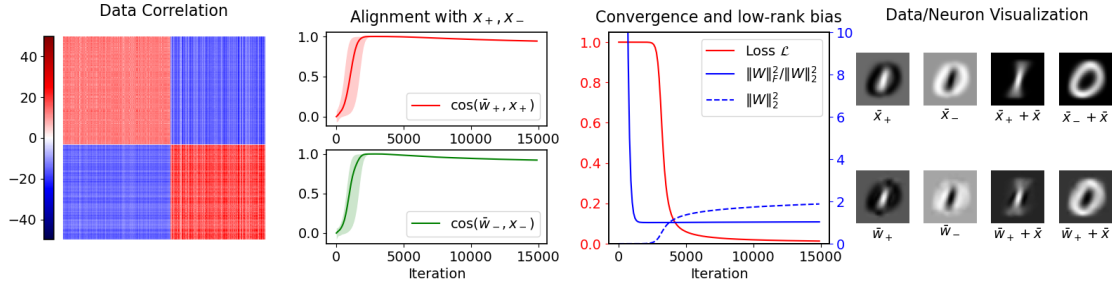


Figure 6: Training two-layer ReLU network under small initialization for binary classification on MNIST digits 0 and 1. The training data is preprocessed to be centered. (First Plot) Data correlation  $[\langle x_i, x_j \rangle]_{ij}$  as a heatmap, where the data are reordered by their label (digit 1 first, then digit 0); (Second Plot) Alignment between neurons and the aggregate positive/negative data  $x_+ = \sum_{i \in \mathcal{I}_+} x_i$ ,  $x_- = \sum_{i \in \mathcal{I}_-} x_i$ . In the top figure, the solid line shows  $\cos(\bar{w}_+, x_+)$  during training, and the shaded region defines the range between  $\min_{j \in \mathcal{V}_+} \cos(w_j, x_+)$  and  $\max_{j \in \mathcal{V}_+} \cos(w_j, x_+)$ . Similarly, in the bottom figure, the solid line shows  $\cos(\bar{w}_-, x_-)$  during training, and the shaded region lies between  $\min_{j \in \mathcal{V}_-} \cos(w_j, x_-)$  and  $\max_{j \in \mathcal{V}_-} \cos(w_j, x_-)$ ; (Third Plot) The loss  $\mathcal{L}$ , the stable rank and the squared spectral norm of  $W$  during training; (Fourth Plot) Visualizing neuron centers  $\bar{w}_+$ ,  $\bar{w}_-$  and data centers  $\bar{x}_+$ ,  $\bar{x}_-$  (at iteration 15000) as grayscale images.  $\bar{x}$  is the mean of the original training data, prior to preprocessing.

we use  $x_i, i \in [n]$ , to denote the preprocessed (centered) data and use  $\bar{x}$  to denote the mean of the original data. Here, we pick digits 1 and 0 for the numerical experiment, and we present additional experiments with different choices of digits in Appendix A.

We build a two-layer ReLU network with  $h = 50$  neurons and initialize all entries of the weights as  $[W]_{ij} \stackrel{i.i.d.}{\sim} \mathcal{N}(0, \alpha)$ ,  $v_j \stackrel{i.i.d.}{\sim} \mathcal{N}(0, \alpha)$ ,  $\forall i \in [n], j \in [h]$  with  $\alpha = 10^{-5}$ . Then we run gradient

descent on both  $W$  and  $v$  with step size  $\eta = 2 \times 10^{-3}$ . Notice that here the weights are not initialized to be balanced as in (3). The numerical results are shown in Figure 6.

**Alignment phase:** Without balancedness, one no longer has  $\text{sign}(v_j(t)) = \text{sign}(v_j(0))$ . With a little abuse of notation, we denote  $\mathcal{V}_+(t) = \{j \in [h] : \text{sign}(v_j(t)) > 0\}$  and  $\mathcal{V}_-(t) = \{j \in [h] : \text{sign}(v_j(t)) < 0\}$ , and we expect that at the end of the alignment phase, neurons in  $\mathcal{V}_+$  are aligned with  $x_+ = \sum_{i \in \mathcal{I}_+} x_i$ , and neurons in  $\mathcal{V}_-$  with  $x_- = \sum_{i \in \mathcal{I}_-} x_i$ . The second plot in Figure 6 shows such an alignment between neurons and  $x_+, x_-$ . In the top part, the red solid line shows  $\cos(\bar{w}_+, x_+)$  during training, where  $\bar{w}_+ = \sum_{j \in \mathcal{V}_+} w_j / |\mathcal{V}_+|$ , and the shaded region defines the range between  $\min_{j \in \mathcal{V}_+} \cos(w_j, x_+)$  and  $\max_{j \in \mathcal{V}_+} \cos(w_j, x_+)$ . Similarly, in the bottom part, the green solid line shows  $\cos(\bar{w}_-, x_-)$  during training, where  $\bar{w}_- = \sum_{j \in \mathcal{V}_-} w_j / |\mathcal{V}_-|$ , and the shaded region delineates the range between  $\min_{j \in \mathcal{V}_-} \cos(w_j, x_-)$  and  $\max_{j \in \mathcal{V}_-} \cos(w_j, x_-)$ . Initially, every neuron is approximately orthogonal to  $x_+, x_-$  due to random initialization. Then all neurons in  $\mathcal{V}_+$  ( $\mathcal{V}_-$ ) start to move towards  $x_+$  ( $x_-$ ) and achieve good alignment after  $\sim 2000$  iterations. When the loss starts to decrease (after  $\sim 3000$  iterations), the alignment drops a little. We conjecture that this is because the dataset does not exactly satisfy our Assumption 1, and the neurons in  $\mathcal{V}_+$  have to fit some negative data, for which  $x_+$  is not the best direction.

**Final convergence:** After  $\sim 3000$  iterations, the norm  $\|W\|_2^2$  starts to grow and the loss decreases, as shown in the third plot in Figure 6. Moreover, the stable rank  $\|W\|_F^2 / \|W\|_2^2$  decreases below 2. For this experiment, we almost have  $\cos(x_+, x_-) \simeq -1$ , thus the neurons in  $\mathcal{V}_+$  (aligned with  $x_+$ ) and those in  $\mathcal{V}_-$  (aligned with  $x_-$ ) are almost co-linear. Therefore, the stable rank  $\|W\|_F^2 / \|W\|_2^2$  is almost 1, as seen from the plot. Finally, at iteration 15000, we visualize the mean neuron  $\bar{w}_+ = \sum_{j \in \mathcal{V}_+} w_j / |\mathcal{V}_+|$ ,  $\bar{w}_- = \sum_{j \in \mathcal{V}_-} w_j / |\mathcal{V}_-|$  as grayscale images, and compare them with  $\bar{x}_+ = x_+ / |\mathcal{I}_+|$ ,  $\bar{x}_- = x_- / |\mathcal{I}_-|$ , showing good alignment. We also show the images when the original data center  $\bar{x}$  is added back.

## 5 Conclusion

This paper studies the problem of training a binary classifier via gradient flow on two-layer ReLU networks under small initialization. We consider a training dataset with well-separated input vectors. A careful analysis of the neurons' directional dynamics allows us to provide an upper bound on the time it takes for all neurons to achieve good alignment with the input data. After the early alignment phase, the loss converges to zero at a  $\mathcal{O}(\frac{1}{t})$  rate, and the weight matrix on the first layer is approximately low-rank. Lastly, the numerical experiment on classifying two digits from the MNIST dataset correlates with our theoretical findings. Future directions include extending our results for gradient descent and considering multi-class classification problems.

## References

- [1] Alex Krizhevsky, Ilya Sutskever, and Geoffrey E Hinton. Imagenet classification with deep convolutional neural networks. In *Advances in neural information processing systems*, pages 1097–1105, 2012.
- [2] Waseem Rawat and Zenghui Wang. Deep convolutional neural networks for image classification: A comprehensive review. *Neural computation*, 29(9):2352–2449, 2017.
- [3] Geoffrey Hinton, Li Deng, Dong Yu, George E Dahl, Abdel-rahman Mohamed, Navdeep Jaitly, Andrew Senior, Vincent Vanhoucke, Patrick Nguyen, Tara N Sainath, et al. Deep neural

- networks for acoustic modeling in speech recognition: The shared views of four research groups. *IEEE Signal processing magazine*, 29(6):82–97, 2012.
- [4] Alex Graves, Abdel-rahman Mohamed, and Geoffrey Hinton. Speech recognition with deep recurrent neural networks. In *2013 IEEE international conference on acoustics, speech and signal processing*, pages 6645–6649. IEEE, 2013.
  - [5] David Silver, Aja Huang, Chris J Maddison, Arthur Guez, Laurent Sifre, George Van Den Driessche, Julian Schrittwieser, Ioannis Antonoglou, Veda Panneershelvam, Marc Lanctot, et al. Mastering the game of go with deep neural networks and tree search. *nature*, 529(7587):484, 2016.
  - [6] Oriol Vinyals, Timo Ewalds, Sergey Bartunov, Petko Georgiev, Alexander Sasha Vezhnevets, Michelle Yeo, Alireza Makhzani, Heinrich Küttler, John Agapiou, Julian Schrittwieser, et al. Starcraft ii: A new challenge for reinforcement learning. *arXiv preprint arXiv:1708.04782*, 2017.
  - [7] Suriya Gunasekar, Blake Woodworth, Srinadh Bhojanapalli, Behnam Neyshabur, and Nathan Srebro. Implicit regularization in matrix factorization. In *Proceedings of the 31st International Conference on Neural Information Processing Systems*, pages 6152–6160, 2017.
  - [8] Sanjeev Arora, Nadav Cohen, Wei Hu, and Yuping Luo. Implicit regularization in deep matrix factorization. *Advances in Neural Information Processing Systems*, 32, 2019.
  - [9] Noam Razin, Asaf Maman, and Nadav Cohen. Implicit regularization in hierarchical tensor factorization and deep convolutional neural networks. In *International Conference on Machine Learning*, pages 18422–18462. PMLR, 2022.
  - [10] Andrew M Saxe, James L McClelland, and Surya Ganguli. Exact solutions to the nonlinear dynamics of learning in deep linear neural network. In *International Conference on Learning Representations*, 2014.
  - [11] Gauthier Gidel, Francis Bach, and Simon Lacoste-Julien. Implicit regularization of discrete gradient dynamics in linear neural networks. In *Advances in Neural Information Processing Systems*, volume 32, pages 3202–3211. Curran Associates, Inc., 2019.
  - [12] Dominik Stöger and Mahdi Soltanolkotabi. Small random initialization is akin to spectral learning: Optimization and generalization guarantees for overparameterized low-rank matrix reconstruction. *Advances in Neural Information Processing Systems*, 34, 2021.
  - [13] Zhiyuan Li, Yuping Luo, and Kaifeng Lyu. Towards resolving the implicit bias of gradient descent for matrix factorization: Greedy low-rank learning. In *International Conference on Learning Representations*, 2021.
  - [14] Hancheng Min, Salma Tarmoun, René Vidal, and Enrique Mallada. On the explicit role of initialization on the convergence and implicit bias of overparametrized linear networks. In *Proceedings of the 38th International Conference on Machine Learning*, volume 139 of *Proceedings of Machine Learning Research*, pages 7760–7768. PMLR, 18–24 Jul 2021.
  - [15] Yuanzhi Li, Tengyu Ma, and Hongyang Zhang. Algorithmic regularization in overparameterized matrix sensing and neural networks with quadratic activations. In Sébastien Bubeck, Vianney Perchet, and Philippe Rigollet, editors, *Proceedings of the 31st Conference On Learning Theory*, volume 75 of *Proceedings of Machine Learning Research*, pages 2–47. PMLR, 06–09 Jul 2018.

- [16] Mahdi Soltanolkotabi, Dominik Stöger, and Changzhi Xie. Implicit balancing and regularization: Generalization and convergence guarantees for overparameterized asymmetric matrix sensing. *arXiv preprint arXiv:2303.14244*, 2023.
- [17] Hartmut Maennel, Olivier Bousquet, and Sylvain Gelly. Gradient descent quantizes relu network features. *arXiv preprint arXiv:1803.08367*, 2018.
- [18] Kaifeng Lyu, Zhiyuan Li, Runzhe Wang, and Sanjeev Arora. Gradient descent on two-layer nets: Margin maximization and simplicity bias. *Advances in Neural Information Processing Systems*, 34:12978–12991, 2021.
- [19] Mary Phuong and Christoph H Lampert. The inductive bias of relu networks on orthogonally separable data. In *International Conference on Learning Representations*, 2021.
- [20] Etienne Boursier, Loucas Pullaud-Vivien, and Nicolas Flammarion. Gradient flow dynamics of shallow relu networks for square loss and orthogonal inputs. In *Advances in Neural Information Processing Systems*, volume 35, pages 20105–20118, 2022.
- [21] Jérôme Bolte, Aris Daniilidis, Olivier Ley, and Laurent Mazet. Characterizations of Łojasiewicz inequalities: subgradient flows, talweg, convexity. *Transactions of the American Mathematical Society*, 362(6):3319–3363, 2010.
- [22] Simon S Du, Wei Hu, and Jason D Lee. Algorithmic regularization in learning deep homogeneous models: Layers are automatically balanced. In *Advances in Neural Information Processing Systems (NeurIPS)*, 2018.
- [23] Sanjeev Arora, Nadav Cohen, and Elad Hazan. On the optimization of deep networks: Implicit acceleration by overparameterization. In *35th International Conference on Machine Learning*, 2018.
- [24] Sanjeev Arora, Nadav Cohen, Noah Golowich, and Wei Hu. A convergence analysis of gradient descent for deep linear neural networks. In *International Conference on Learning Representations*, 2018.
- [25] Chulhee Yun, Shankar Krishnan, and Hossein Mobahi. A unifying view on implicit bias in training linear neural networks. In *International Conference on Learning Representations*, 2020.
- [26] Thien Le and Stefanie Jegelka. Training invariances and the low-rank phenomenon: beyond linear networks. In *International Conference on Learning Representations*, 2022.

## A Additional Experiments

### A.1 Additional experiments on MNIST dataset

We use exactly the same experimental setting as in the main paper and only use a different pair of digits. The results are as follows:

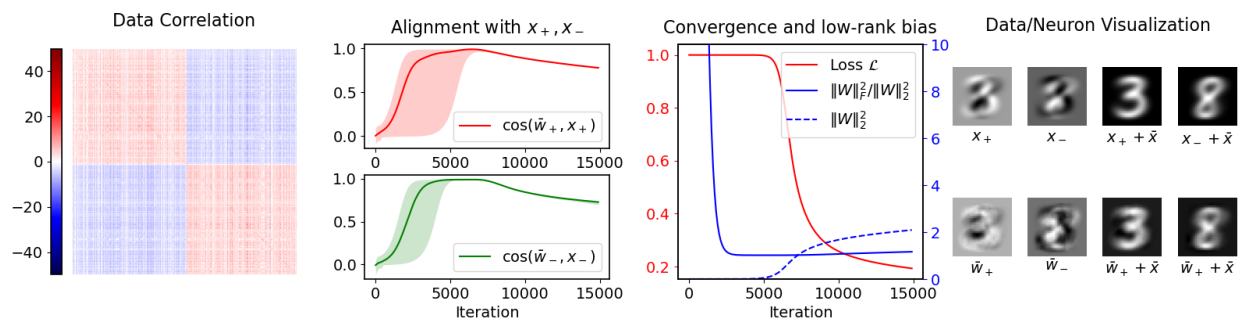


Figure 7: Binary classification on MNIST Digits 3 and 8.

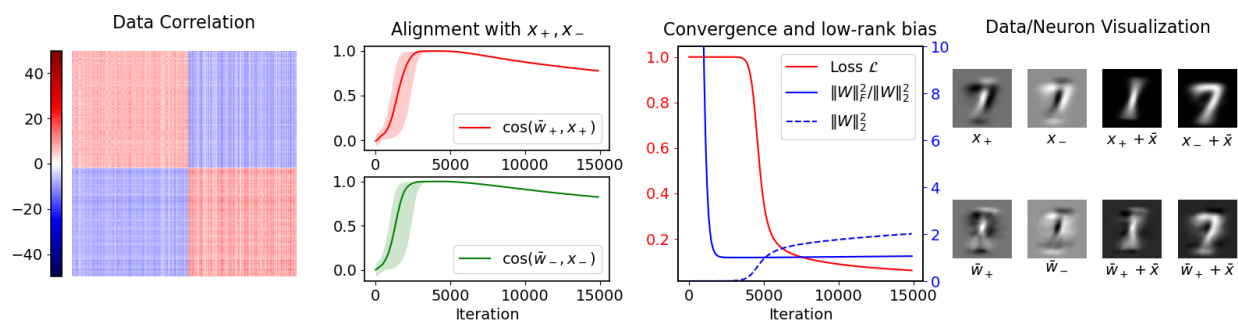


Figure 8: Binary classification on MNIST Digits 1 and 7.

### A.2 Error bars

We provide here error bars for the numerical experiments in Section 4. We run each experiment 20 times and report the mean loss curve below, the shaded region presents the values within 3 times the standard deviation.

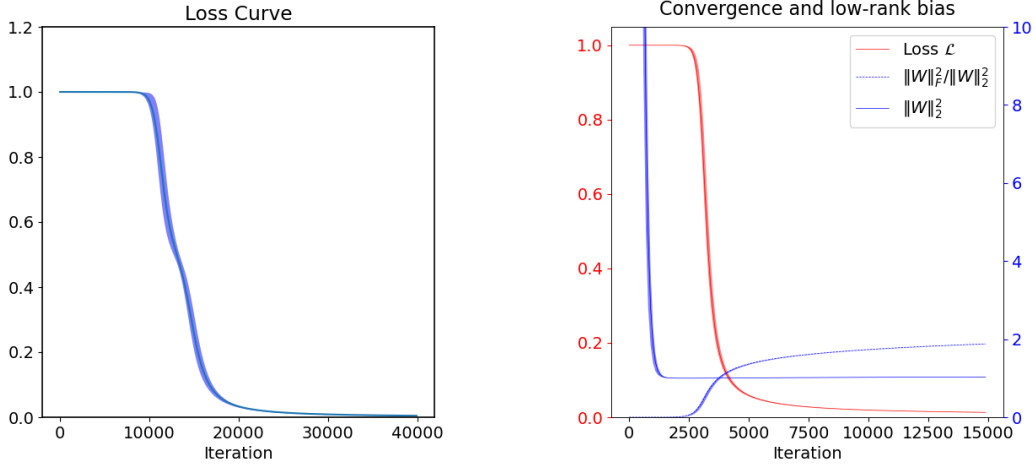


Figure 9: Errorbar for our illustrative exam-ple  
Figure 10: Errorbar for our experiment on MNIST data

## B Proof of Lemma 1

The following property of the exponential loss  $\ell$  will be used throughout the Appendix for proofs of several results:

**Lemma 2.** *For exponential loss  $\ell$ , we have*

$$|-\nabla_{\hat{y}}\ell(y, \hat{y}) - y| \leq 2|\hat{y}|, \forall y \in \{+1, -1\}, \quad \forall |\hat{y}| \leq 1. \quad (10)$$

*Proof.*

$$\begin{aligned} |-\nabla_{\hat{y}}\ell(y, \hat{y}) - y| &= |y \exp(-y\hat{y}) - y| \\ &\leq |y| |\exp(-y\hat{y}) - 1| \\ &\leq |\exp(-y\hat{y}) - 1| \leq 2|\hat{y}|, \end{aligned}$$

where the last inequality is due to the fact that  $2x \geq \max\{1 - \exp(-x), \exp(x) - 1\}, \forall x \in [0, 1]$ .  $\square$

### B.1 Formal statement

Denote:  $X_{\max} = \max_i \|x_i\|, W_{\max} = \max_j \|[W_0]_{:,j}\|$ . The formal statement of Lemma 1 is as follow:

**Lemma 1.** *Given some initialization from (3), for any  $\epsilon \leq \frac{1}{4\sqrt{h}X_{\max}W_{\max}^2}$ , then any solution to the gradient flow dynamics (2) satisfies that  $\forall t \leq T = \frac{1}{4nX_{\max}} \log \frac{1}{\sqrt{h\epsilon}}$ ,*

$$\max_j \left\| \frac{d}{dt} \frac{w_j(t)}{\|w_j(t)\|} - \text{sign}(v_j(0)) \mathcal{P}_{w_j(t)} x_a(w_j(t)) \right\| \leq 4\epsilon n \sqrt{h} X_{\max}^2 W_{\max}^2.$$

Lemma 1 is a direct result of the following two lemmas.

**Lemma 3.** *Given some initialization in (3), then for any  $\epsilon \leq \frac{1}{4\sqrt{h}X_{\max}W_{\max}^2}$ , any solution to the gradient flow dynamics (2) satisfies*

$$\max_j \|w_j(t)\|^2 \leq \frac{2\epsilon W_{\max}^2}{\sqrt{h}}, \quad \max_i |f(x_i; W(t), v(t))| \leq 2\epsilon \sqrt{h} X_{\max} W_{\max}^2, \quad (11)$$

$$\forall t \leq \frac{1}{4nX_{\max}} \log \frac{1}{\sqrt{h\epsilon}}.$$

**Lemma 4.** Consider any solution to the gradient flow dynamic (2) starting from initialization (3). Whenever  $\max_i |f(x_i; W, v)| \leq 1$ , we have,  $\forall i \in [n]$ ,

$$\left\| \frac{d}{dt} \frac{w_j}{\|w_j\|} - \text{sign}(v_j(0)) \left( I - \frac{w_j w_j^\top}{\|w_j\|^2} \right) \left( \sum_{i: \langle x_i, w_j \rangle > 0} y_i x_i \right) \right\| \leq 2nX_{\max} \max_i |f(x_i; W, v)|. \quad (12)$$

## B.2 Proof of Lemma 3 and Lemma 4

*Proof of Lemma 3.* Under gradient flow, we have

$$\frac{d}{dt} w_j = - \sum_{i=1}^n \mathbb{1}_{\langle x_i, w_j \rangle \geq 0} \nabla_{\hat{y}} \ell(y_i, f(x_i; W, v)) x_i v_j. \quad (13)$$

Balanced initialization enforces  $v_j = \text{sign}(v_j(0)) \|w_j\|$ , hence

$$\frac{d}{dt} w_j = - \sum_{i=1}^n \mathbb{1}_{\langle x_i, w_j \rangle \geq 0} \nabla_{\hat{y}} \ell(y_i, f(x_i; W, v)) x_i \text{sign}(v_j(0)) \|w_j\|. \quad (14)$$

Let  $T := \inf\{t : \max_i |f(x_i; W(t), v(t))| > 2\epsilon\sqrt{h}X_{\max}W_{\max}^2\}$ , then  $\forall t \leq T, j \in [h]$ , we have

$$\begin{aligned} \frac{d}{dt} \|w_j\|^2 &= \left\langle w_j, \frac{d}{dt} w_j \right\rangle \\ &= -2 \sum_{i=1}^n \mathbb{1}_{\langle x_i, w_j \rangle \geq 0} \nabla_{\hat{y}} \ell(y_i, f(x_i; W, v)) \langle x_i, w_j \rangle \text{sign}(v_j(0)) \|w_j\| \\ &\leq 2 \sum_{i=1}^n |\nabla_{\hat{y}} \ell(y_i, f(x_i; W, v))| |\langle x_i, w_j \rangle| \|w_j\| \\ &\leq 2 \sum_{i=1}^n (|y_i| + 2|f(x_i; W, v)|) |\langle x_i, w_j \rangle| \|w_j\| && \text{(by Lemma 2)} \\ &\leq 2 \sum_{i=1}^n (1 + 4\epsilon\sqrt{h}X_{\max}W_{\max}^2) |\langle x_i, w_j \rangle| \|w_j\| && \text{(Since } t \leq T) \\ &\leq 2 \sum_{i=1}^n (1 + 4\epsilon\sqrt{h}X_{\max}W_{\max}^2) \|x_i\| \|w_j\|^2 \\ &\leq 2n(X_{\max} + 4\epsilon\sqrt{h}X_{\max}^2W_{\max}^2) \|w_j\|^2. \end{aligned} \quad (15)$$

Let  $\tau_j := \inf\{t : \|w_j(t)\|^2 > \frac{2\epsilon W_{\max}^2}{\sqrt{h}}\}$ , and let  $j^* := \arg \min_j \tau_j$ , then  $\tau_{j^*} = \min_j \tau_j \leq T$  due to the fact that

$$|f(x_i; W, v)| = \left| \sum_{j \in [h]} \mathbb{1}_{\langle w_j, x_i \rangle > 0} v_j \langle w_j, x_i \rangle \right| \leq \sum_{j \in [h]} \|w_j\|^2 \|x_i\| \leq hX_{\max} \max_{j \in [h]} \|w_j\|^2,$$

which implies " $|f(x_i; W(t), v(t))| > 2\epsilon\sqrt{h}X_{\max}W_{\max}^2 \Rightarrow \exists j, s.t. \|w_j(t)\|^2 > \frac{2\epsilon W_{\max}^2}{\sqrt{h}}$ ".



Then for  $t \leq \tau_{j^*}$ , we have

$$\frac{d}{dt} \|w_{j^*}\|^2 \leq 2n(X_{\max} + 4\epsilon\sqrt{h}X_{\max}^2W_{\max}^2) \|w_{j^*}\|^2. \quad (16)$$

By Grönwall's inequality, we have  $\forall t \leq \tau_{j^*}$

$$\begin{aligned} \|w_{j^*}(t)\|^2 &\leq \exp\left(2n(X_{\max} + 4\epsilon\sqrt{h}X_{\max}^2W_{\max}^2)t\right) \|w_{j^*}(0)\|^2, \\ &= \exp\left(2n(X_{\max} + 4\epsilon\sqrt{h}X_{\max}^2W_{\max}^2)t\right) \epsilon^2 \|[W_0]_{:,j^*}\|^2 \\ &\leq \exp\left(2n(X_{\max} + 4\epsilon\sqrt{h}X_{\max}^2W_{\max}^2)t\right) \epsilon^2 W_{\max}^2. \end{aligned}$$

Suppose  $\tau_{j^*} < \frac{1}{4nX_{\max}} \log\left(\frac{1}{\sqrt{h}\epsilon}\right)$ , then by the continuity of  $\|w_{j^*}(t)\|^2$ , we have

$$\begin{aligned} \frac{2\epsilon W_{\max}^2}{\sqrt{h}} &\leq \|w_{j^*}(\tau_{j^*})\|^2 \leq \exp\left(2n(X_{\max} + 4\epsilon\sqrt{h}X_{\max}^2W_{\max}^2)\tau_{j^*}\right) \epsilon^2 W_{\max}^2 \\ &\leq \exp\left(2n(X_{\max} + 4\epsilon\sqrt{h}X_{\max}^2W_{\max}^2)\frac{1}{4nX_{\max}} \log\left(\frac{1}{\sqrt{h}\epsilon}\right)\right) \epsilon^2 W_{\max}^2 \\ &\leq \exp\left(\frac{1 + 4\epsilon\sqrt{h}X_{\max}W_{\max}^2}{2} \log\left(\frac{1}{\sqrt{h}\epsilon}\right)\right) \epsilon^2 W_{\max}^2 \\ &\leq \exp\left(\log\left(\frac{1}{\sqrt{h}\epsilon}\right)\right) \epsilon^2 W_{\max}^2 = \frac{\epsilon W_{\max}^2}{\sqrt{h}}, \end{aligned}$$

which leads to a contradiction  $2\epsilon \leq \epsilon$ . Therefore, one must have  $T \geq \tau_{j^*} \geq \frac{1}{4nX_{\max}} \log\left(\frac{1}{\sqrt{h}\epsilon}\right)$ . This finishes the proof.  $\square$

*Proof of Lemma 4.* As we showed in the proof for Lemma 3, under balanced initialization,

$$\frac{d}{dt} w_j = - \sum_{i=1}^n \mathbb{1}_{\langle x_i, w_j \rangle \geq 0} \nabla_{\hat{y}} \ell(y_i, f(x_i; W, v)) x_i \text{sign}(v_j(0)) \|w_j\|. \quad (17)$$

Then for any  $i \in [n]$ ,

$$\begin{aligned} \frac{d}{dt} \frac{w_j}{\|w_j\|} &= -\text{sign}(v_j(0)) \sum_{i=1}^n \mathbb{1}_{\langle x_i, w_j \rangle > 0} \nabla_{\hat{y}} \ell(y_i, f(x_i; W, v)) \left(x_i - \frac{\langle x_i, w_j \rangle}{\|w_j\|^2} w_j\right) \\ &= -\text{sign}(v_j(0)) \sum_{i: \langle x_i, w_j \rangle > 0} \nabla_{\hat{y}} \ell(y_i, f(x_i; W, v)) \left(x_i - \frac{\langle x_i, w_j \rangle}{\|w_j\|^2} w_j\right) \\ &= -\text{sign}(v_j(0)) \left(I - \frac{w_j w_j^\top}{\|w_j\|^2}\right) \left(\sum_{i: \langle x_i, w_j \rangle > 0} \nabla_{\hat{y}} \ell(y_i, f(x_i; W, v)) x_i\right). \end{aligned}$$

Therefore, whenever  $\max_i |f(x_i; W, v)| \leq 1$ ,

$$\begin{aligned}
& \left\| \frac{d}{dt} \frac{w_j}{\|w_j\|} - \text{sign}(v_j(0)) \left( I - \frac{w_j w_j^\top}{\|w_j\|^2} \right) \left( \sum_{i: \langle x_i, w_j \rangle > 0} y_i x_i \right) \right\| \\
&= \left\| \text{sign}(v_j(0)) \left( \sum_{i: \langle x_i, w_j \rangle > 0} (\nabla_{\hat{y}} \ell(y_i, f(x_i; W, v)) + y_i) x_i \right) \right\| \\
&\leq \sum_{i=1}^n |\nabla_{\hat{y}} \ell(y_i, f(x_i; W, v)) + y_i| \cdot \|x_i\| \\
&\leq \sum_{i=1}^n 2|f(x_i; W, v)| \cdot \|x_i\| \leq 2nM_x \max_i |f(x_i; W, v)|. \tag{18}
\end{aligned}$$

□

## C Proof for Theorem 1: Early Alignment Phase

We break the proof of Theorem 1 into two parts: In Appendix C we prove the first part regarding directional convergence. Then in Appendix D we prove the remaining statement on final convergence and low-rank bias.

### C.1 Auxiliary lemmas

The first several Lemmas concern mostly some conic geometry given the data assumption:

Consider the following conic hull

$$K = \mathcal{CH}(\{x_i y_i, i \in [n]\}) = \left\{ \sum_{i=1}^n a_i x_i y_i : a_i \geq 0, i \in [n] \right\}. \quad (19)$$

It is clear that  $x_i y_i \in K, \forall i$ , and  $x_a(w) \in K, \forall w$ . The following lemma shows any pair of vectors in  $K$  is  $\mu$ -coherent.

**Lemma 5.**  $\cos(z_1, z_2) \geq \mu, \forall 0 \neq z_1, z_2 \in K$ .

*Proof.* Since  $z_1, z_2 \in K$ , we let  $z_1 = \sum_{i=1}^n x_i y_i a_{1i}$ , and  $z_2 = \sum_{j=1}^n x_j y_j a_{2j}$ , where  $a_{1i}, a_{2j} \geq 0$  but not all of them.

$$\begin{aligned} \cos(z_1, z_2) &= \frac{1}{\|z_1\| \|z_2\|} \langle z_1, z_2 \rangle = \frac{1}{\|z_1\| \|z_2\|} \sum_{i,j \in [n]} a_{1i} a_{2j} \langle x_i y_i, x_j y_j \rangle \\ &= \frac{\sum_{i,j \in [n]} \|x_i\| \|x_j\| a_{1i} a_{2j} \mu}{\|z_1\| \|z_2\|} \geq \mu, \end{aligned}$$

where the last inequality is due to

$$\|z_1\| \|z_2\| \leq \left( \sum_{i=1}^n \|x_i\| a_{1i} \right) \left( \sum_{j=1}^n \|x_j\| a_{2j} \right) = \sum_{i,j \in [n]} \|x_i\| \|x_j\| a_{1i} a_{2j}.$$

□

The following lemma is some basic results regarding  $\mathcal{S}_+$  and  $\mathcal{S}_-$ :

**Lemma 6.**  $\mathcal{S}_+$  and  $\mathcal{S}_-$  are convex cones (excluding the origin).

*Proof.* Since  $\mathbb{1}_{\langle x_i, z \rangle} = \mathbb{1}_{\langle x_i, az \rangle}, \forall i \in [n], a > 0$ ,  $\mathcal{S}_+, \mathcal{S}_-$  are cones. Moreover,  $\langle x_i, z_1 \rangle > 0$  and  $\langle x_i, z_2 \rangle > 0$  implies  $\langle x_i, a_1 z_1 + a_2 z_2 \rangle > 0, \forall a_1, a_2 > 0$ , thus  $\mathcal{S}_+, \mathcal{S}_-$  are convex cones. □

Now we consider the complete metric space  $\mathbb{S}^{D-1}$  (w.r.t.  $\arccos(\langle \cdot, \cdot \rangle)$ ) and we are interested in its subsets  $K \cap \mathbb{S}^{D-1}, \mathcal{S}_+ \cap \mathbb{S}^{D-1}$ , and  $\mathcal{S}_- \cap \mathbb{S}^{D-1}$ . First, we have (we use  $\text{Int}(S)$  to denote the interior of  $S$ )

**Lemma 7.**  $K \cap \mathbb{S}^{D-1} \subset \text{Int}(\mathcal{S}_+ \cap \mathbb{S}^{D-1})$ , and  $-K \cap \mathbb{S}^{D-1} \subset \text{Int}(\mathcal{S}_- \cap \mathbb{S}^{D-1})$

*Proof.* Consider any  $x_c = \sum_{j=1}^n a_j x_j y_j \in K \cap \mathbb{S}^{D-1}$ , For any  $x_i, y_i, i \in [n]$ , we have

$$\begin{aligned} \langle x_c, x_i \rangle &= \sum_{j=1}^n a_j \|x_j\| \left\langle \frac{x_j y_j}{\|x_j\|}, \frac{x_i y_i}{\|x_i\|} \right\rangle \frac{\|x_i\|}{y_i} \\ &\geq \mu y_i \|x_i\| \sum_{j=1}^n a_j \|x_j\| \begin{cases} \geq \mu X_{\min} > 0, & y_i > 0 \\ \leq -\mu X_{\min} < 0, & y_i < 0 \end{cases}. \end{aligned}$$

Depending on the sign of  $y_i$ , we have either

$$\langle x_c, x_i \rangle = \sum_{j=1}^n a_j \|x_j\| \left\langle \frac{x_j y_j}{\|x_j\|}, \frac{x_i y_i}{\|x_i\|} \right\rangle \frac{\|x_i\|}{y_i} \geq \mu \frac{\|x_i\|}{y_i} \sum_{j=1}^n a_j \|x_j\| \geq \mu X_{\min} > 0, \quad (y_i = +1)$$

or

$$\langle x_c, x_i \rangle = \sum_{j=1}^n a_j \|x_j\| \left\langle \frac{x_j y_j}{\|x_j\|}, \frac{x_i y_i}{\|x_i\|} \right\rangle \frac{\|x_i\|}{y_i} \leq \mu \frac{\|x_i\|}{y_i} \sum_{j=1}^n a_j \|x_j\| \leq -\mu X_{\min} < 0, \quad (y_i = -1)$$

where we use the fact that  $1 = \|x_c\| = \|\sum_{j=1}^n a_j x_j y_j\| \leq \sum_{j=1}^n a_j \|x_j\|$ . This already tells us  $x_c \in \mathcal{S}_+ \cap \mathbb{S}^{D-1}$ .

Since  $f_i(z) = \langle z, x_i \rangle$  is a continuous function of  $z \in \mathbb{S}^{D-1}$ . There exists an open ball  $\mathcal{B}(x_c, \delta_i)$  centered at  $x_c$  with some radius  $\delta_i > 0$ , such that  $\forall z \in \mathcal{B}(x_c, \delta_i)$ , one have  $|f_i(z) - f_i(x_c)| \leq \frac{\mu X_{\min}}{2}$ , which implies

$$\langle z, x_i \rangle \begin{cases} \geq \mu X_{\min}/2 > 0, & y_i > 0 \\ \leq -\mu X_{\min}/2 < 0, & y_i < 0 \end{cases}.$$

Hence  $\bigcap_{i=1}^n \mathcal{B}\left(\frac{x_c}{\|x_c\|}, \delta_i\right) \in \mathcal{S}_+ \cap \mathbb{S}^{D-1}$ . Therefore,  $x_c \in \text{Int}(\mathcal{S}_+ \cap \mathbb{S}^{D-1})$ . This suffices to show  $K \cap \mathbb{S}^{D-1} \subset \text{Int}(\mathcal{S}_+ \cap \mathbb{S}^{D-1})$ . The other statement  $-K \cap \mathbb{S}^{D-1} \subset \text{Int}(\mathcal{S}_- \cap \mathbb{S}^{D-1})$  is proved similarly.  $\square$

The following two lemmas are some direct results of Lemma 7.

**Lemma 8.**  $\exists \zeta_1 > 0$  such that

$$\mathcal{S}_{x_+}^{\zeta_1} \subset \mathcal{S}_+, \quad \mathcal{S}_{x_-}^{\zeta_1} \subset \mathcal{S}_-, \quad (20)$$

where  $\mathcal{S}_x^\zeta := \{z \in \mathbb{R}^D : \cos(z, x) \geq \sqrt{1 - \zeta}\}$ .

*Proof.* By Lemma 7,  $\frac{x_+}{\|x_+\|} \in K \subset \text{Int}(\mathcal{S}_+)$ . Since  $\mathbb{S}^{D-1}$  is a complete metric space (w.r.t  $\arccos(\cdot, \cdot)$ ), there exists a open ball centered at  $\frac{x_+}{\|x_+\|}$  of some radius  $\arccos(\sqrt{1 - \zeta_1})$  that is a subset of  $\mathcal{S}_+$ , from which one can show  $\mathcal{S}_{x_+}^{\zeta_1} \subset \mathcal{S}_+$ . The other statement  $\mathcal{S}_{x_-}^{\zeta_1} \subset \mathcal{S}_-$  simply comes from the fact that  $x_+ = -x_-$  and  $\text{Int}(\mathcal{S}_+) = -\text{Int}(\mathcal{S}_-)$ .  $\square$

**Lemma 9.**  $\exists \xi > 0$ , such that

$$\sup_{x_1 \in K \cap \mathbb{S}^{D-1}, x_2 \in (\mathcal{S}_+ \cap \mathbb{S}^{D-1})^c \cap (\mathcal{S}_- \cap \mathbb{S}^{D-1})^c} |\cos(x_1, x_2)| \leq \sqrt{1 - \xi}. \quad (21)$$

( $S^c$  here is defined to be  $\mathbb{S}^{D-1} - S$ , the set complement w.r.t. complete space  $\mathbb{S}^{D-1}$ )

*Proof.* Notice that

$$\sup_{x_1 \in K \cap \mathbb{S}^{D-1}, x_2 \in (\text{Int}(\mathcal{S}_+ \cap \mathbb{S}^{D-1}))^c} \langle x_1, x_2 \rangle = \inf_{x_1 \in K \cap \mathbb{S}^{D-1}, x_2 \in (\text{Int}(\mathcal{S}_+ \cap \mathbb{S}^{D-1}))^c} \arccos \langle x_1, x_2 \rangle .$$

Since  $\mathbb{S}^{D-1}$  is a complete metric space (w.r.t  $\arccos \langle \cdot, \cdot \rangle$ ) and  $K \cap \mathbb{S}^{D-1}$  and  $x_2 \in (\text{Int}(\mathcal{S}_+ \cap \mathbb{S}^{D-1}))^c$  are two of its compact subsets. Suppose

$$\inf_{x_1 \in K \cap \mathbb{S}^{D-1}, x_2 \in x_2 \in (\text{Int}(\mathcal{S}_+ \cap \mathbb{S}^{D-1}))^c} \arccos \langle x_1, x_2 \rangle = 0 ,$$

then  $\exists x_1 \in K \cap \mathbb{S}^{D-1}, x_2 \in (\text{Int}(\mathcal{S}_+ \cap \mathbb{S}^{D-1}))^c$  such that  $\arccos \langle x_1, x_2 \rangle = 0$ , i.e.,  $x_1 = x_2$ , which contradicts the fact that  $K \cap \mathbb{S}^{D-1} \subseteq \text{Int}(\mathcal{S}_+ \cap \mathbb{S}^{D-1})$  (Lemma 7). Therefore, we have the infimum strictly larger than zero, then

$$\sup_{x_1 \in K \cap \mathbb{S}^{D-1}, x_2 \in (\mathcal{S}_+ \cap \mathbb{S}^{D-1})^c} \langle x_1, x_2 \rangle \leq \sup_{x_1 \in K \cap \mathbb{S}^{D-1}, x_2 \in (\text{Int}(\mathcal{S}_+ \cap \mathbb{S}^{D-1}))^c} \langle x_1, x_2 \rangle < 1 . \quad (22)$$

Similarly, one can show that

$$\sup_{x_1 \in -K \cap \mathbb{S}^{D-1}, x_2 \in (\mathcal{S}_- \cap \mathbb{S}^{D-1})^c} \langle x_1, x_2 \rangle < 1 . \quad (23)$$

Finally, find  $\xi < 1$  such that

$$\max \left\{ \sup_{x_1 \in K \cap \mathbb{S}^{D-1}, x_2 \in (\mathcal{S}_+ \cap \mathbb{S}^{D-1})^c} \langle x_1, x_2 \rangle, \sup_{x_1 \in -K \cap \mathbb{S}^{D-1}, x_2 \in (\mathcal{S}_- \cap \mathbb{S}^{D-1})^c} \langle x_1, x_2 \rangle \right\} = \sqrt{1 - \xi} ,$$

then for any  $x_1 \in K \cap \mathbb{S}^{D-1}$  and  $x_2 \in (\mathcal{S}_+ \cap \mathbb{S}^{D-1})^c \cap (\mathcal{S}_- \cap \mathbb{S}^{D-1})^c$ , we have

$$-\sqrt{1 - \xi} \leq \langle x_1, x_2 \rangle \leq \sqrt{1 - \xi} ,$$

which is the desired result.  $\square$

The remaining two lemmas are technical but extensively used in the main proof.

**Lemma 10.** Consider any solution to the gradient flow dynamic (2) starting from initialization (3). Let  $x_r \in \mathbb{S}^{n-1}$  be some reference direction, we define

$$\psi_{rj} = \left\langle x_r, \frac{w_j}{\|w_j\|} \right\rangle, \psi_{ra} = \left\langle x_r, \frac{x_a(w_j)}{\|x_a(w_j)\|} \right\rangle, \psi_{aj} = \left\langle \frac{w_j}{\|w_j\|}, \frac{x_a(w_j)}{\|x_a(w_j)\|} \right\rangle, \quad (24)$$

where  $x_a(w_j) = \sum_{i: \langle x_i, w_j \rangle > 0} y_i x_i$ .

Whenever  $\max_i |f(x_i; W, v)| \leq 1$ , we have

$$\left| \frac{d}{dt} \psi_{rj} - \text{sign}(v_j(0)) (\psi_{ra} - \psi_{rj} \psi_{aj}) \|x_a(w_j)\| \right| \leq 2n X_{\max} \max_i |f(x_i; W, v)| . \quad (25)$$

*Proof.* A simple application of Lemma 4, together with Cauchy-Schwartz:

$$\begin{aligned} & \left| \frac{d}{dt} \psi_{rj} - \text{sign}(v_j(0)) (\psi_{ra} - \psi_{rj} \psi_{aj}) \|x_a(w_j)\| \right| \\ &= \left| x_r^\top \left( \frac{d}{dt} \frac{w_j}{\|w_j\|} - \text{sign}(v_j(0)) \left( I - \frac{w_j w_j^\top}{\|w_j\|^2} \right) \left( \sum_{i: \langle x_i, w_j \rangle > 0} y_i x_i \right) \right) \right| \leq 2n X_{\max} \max_i |f(x_i; W, v)| . \end{aligned}$$

$\square$

**Lemma 11.**

$$\|x_a(w)\| \geq \sqrt{\mu} n_a(w) X_{\min}, \quad (26)$$

where  $n_a(w) = |\{i \in [n] : \langle x_i, w \rangle > 0\}|$ .

*Proof.* Let  $\mathcal{I}_a(w)$  denote  $\{i \in [n] : \langle x_i, w \rangle > 0\}$ , then

$$\begin{aligned} \|x_a(w)\| &= \left\| \sum_{i: \langle x_i, w \rangle > 0} x_i y_i \right\| = \sqrt{\sum_{i \in \mathcal{I}_a(w)} \|x_i\|^2 y_i^2 + \sum_{i, j \in \mathcal{I}_a(w), i < j} \|x_i\| \|x_j\| \left\langle \frac{x_i y_i}{\|x_i\|}, \frac{x_j y_j}{\|x_j\|} \right\rangle} \\ &\geq \sqrt{\sum_{i \in \mathcal{I}_a(w)} \|x_i\|^2 y_i^2 + \sum_{i, j \in \mathcal{I}_a(w), i < j} \|x_i\| \|x_j\| |y_i| |y_j| \mu} \\ &\geq \sqrt{n_a(w) X_{\min}^2 + \mu n_a(w) (n_a(w) - 1) X_{\min}^2} \\ &\geq \sqrt{n_a(w) (1 + \mu (n_a(w) - 1))} X_{\min} \\ &\geq \sqrt{\mu} n_a(w) X_{\min}. \end{aligned}$$

□

## C.2 Proof for early alignment phase

*Proof of Theorem 1: First Part.* Given some initialization in (3), by Assumption 2,  $\exists \zeta_2 > 0$ , such that

$$\max_{j \in \mathcal{V}_+} \cos(w_j(0), x_-) < \sqrt{1 - \zeta_2}, \quad \max_{j \in \mathcal{V}_-} \cos(w_j(0), x_+) < \sqrt{1 - \zeta_2}. \quad (27)$$

We define  $\zeta := \max\{\zeta_1, \zeta_2\}$ , where  $\zeta_1$  is from Lemma 8. In addition, by Lemma 9,  $\exists \xi > 0$ , such that

$$\sup_{x_1 \in K \cap \mathcal{S}^{D-1}, x_2 \in \mathcal{S}_-^c \cap \mathcal{S}_+^c \cap \mathcal{S}^{D-1}} |\cos(x_1, x_2)| \leq \sqrt{1 - \xi}. \quad (28)$$

We pick a initialization scale  $\epsilon$  that satisfies:

$$\epsilon \leq \min \left\{ \frac{\min\{\mu, \zeta, \xi\} \sqrt{\mu} X_{\min}}{4\sqrt{h} n X_{\max}^2 W_{\max}^2}, \frac{1}{\sqrt{h}} \exp \left( -\frac{64n X_{\max}}{\min\{\zeta, \xi\} \sqrt{\mu} X_{\min}} \log n \right) \right\} \leq \frac{1}{4\sqrt{h} X_{\max} W_{\max}^2}. \quad (29)$$

By Lemma 3,  $\forall t \leq T = \frac{1}{4n X_{\max}} \log \frac{1}{\sqrt{h\epsilon}}$ , we have

$$\max_i |f(x_i; W, v)| \leq \frac{\min\{\mu, \zeta, \xi\} \sqrt{\mu} X_{\min}}{4n X_{\max}}, \quad (30)$$

which is the key to analyzing the alignment phase. For the sake of simplicity, we only discuss the analysis of neurons in  $\mathcal{V}_+$  here, the proof for neurons in  $\mathcal{V}_-$  is almost identical.

**Activation pattern evolution:** Pick any  $w_j$  in  $\mathcal{V}_+$  and pick  $x_r = x_i y_i$  for some  $i \in [n]$ , and consider the case when  $\langle w_j, x_i \rangle = 0$ . From Lemma 10, we have

$$\left| \frac{d}{dt} \psi_{rj} - (\psi_{ra} - \psi_{rj} \psi_{aj}) \|x_a(w_j)\| \right| \leq 2n X_{\max} \max_i |f(x_i; W, v)|.$$

$\langle w_j, x_i \rangle = 0$  implies  $\psi_{rj} = \left\langle \frac{x_i y_i}{\|x_i\|}, \frac{w_j}{\|w_j\|} \right\rangle = 0$ , thus we have

$$\left| \frac{d}{dt} \psi_{rj} |_{\langle w_j, x_i \rangle = 0} - \psi_{ra} \|x_a(w_j)\| \right| \leq 2n X_{\max} \max_i |f(x_i; W, v)|.$$

Then whenever  $w_j \notin \mathcal{S}_{\text{dead}}$ , we have

$$\begin{aligned}
\frac{d}{dt}\psi_{rj}|_{\langle w_j, x_i \rangle = 0} &\geq \psi_{ra}\|x_a(w_j)\| - 2nX_{\max} \max_i |f(x_i; W, v)| \\
&\geq \mu\|x_a(w_j)\| - 2nX_{\max} \max_i |f(x_i; W, v)| && \text{(by Lemma 5)} \\
&\geq \mu^{3/2}X_{\min} - 2nX_{\max} \max_i |f(x_i; W, v)| && \text{(by Lemma 11)} \\
&\geq \mu^{3/2}X_{\min}/2 > 0. && \text{(by (30))}
\end{aligned}$$

This is precisely (8) in Section 3.2.

**Bound on activation transitions and duration:** Next we show that if at time  $t_0 < T$ ,  $w_j(t_0) \notin \mathcal{S}_+ \cup \mathcal{S}_{\text{dead}}$ , and the activation pattern of  $w_j$  is  $\mathbb{1}_{\langle x_i, w_j(t_0) \rangle > 0}$ , then  $\mathbb{1}_{\langle x_i, w_j(t_0 + \Delta t) \rangle > 0} \neq \mathbb{1}_{\langle x_i, w_j(t_0) \rangle > 0}$ , where  $\Delta t = \frac{4}{\min\{\zeta, \xi\}\sqrt{\mu}X_{\min}n_a(w_j(t_0))}$  and  $n_a(w_j(t_0))$  is defined in Lemma 11 as long as  $t_0 + \Delta t < T$  as well. That is, during the alignment phase  $[0, T]$ ,  $w_j$  must change its activation pattern within  $\Delta t$  time. There are two cases:

- The first case is when  $w_j(t_0) \in \mathcal{S}_+^c \cap \mathcal{S}_-^c \cap \mathcal{S}_{\text{dead}}^c$ . In this case, suppose that  $\mathbb{1}_{\langle x_i, w_j(t_0 + \tau) \rangle > 0} = \mathbb{1}_{\langle x_i, w_j(t_0) \rangle > 0}, \forall 0 \leq \tau \leq \Delta t$ , i.e.  $w_j$  fixes its activation during  $[t_0, t_0 + \Delta t]$ , then we have  $x_a(w_j(t_0 + \tau)) = x_a(w_j(t_0)), \forall 0 \leq \tau \leq \Delta t$ . Let us pick  $x_r = x_a(w_j(t_0))$ , then Lemma 10 leads to

$$\left| \frac{d}{dt} \cos(w_j, x_a(w_j)) - (1 - \cos^2(w_j, x_a(w_j))) \|x_a(w_j)\| \right| \leq 2nX_{\max} \max_i |f(x_i; W, v)|.$$

Since  $x_a(w_j)$  is fixed, we have  $\forall t \in [t_0, t_0 + \Delta t]$ ,

$$\left| \frac{d}{dt} \cos(w_j, x_a(w_j(t_0))) - (1 - \cos^2(w_j, x_a(w_j(t_0)))) \|x_a(w_j(t_0))\| \right| \leq 2nX_{\max} \max_i |f(x_i; W, v)|,$$

$$\begin{aligned}
\frac{d}{dt} \cos(w_j, x_a(w_j(t_0))) &\geq (1 - \cos^2(w_j, x_a(w_j(t_0)))) \|x_a(w_j(t_0))\| \\
&\quad - 2nX_{\max} \max_i |f(x_i; W, v)| \\
&\geq \xi \|x_a(w_j(t_0))\| - 2nX_{\max} \max_i |f(x_i; W, v)| && \text{(by (28))} \\
&\geq \xi \sqrt{\mu} n_a(w_j(t_0)) X_{\min} - 2nX_{\max} \max_i |f(x_i; W, v)| && \text{(by Lemma 11)} \\
&\geq \xi \sqrt{\mu} n_a(w_j(t_0)) X_{\min}/2. && \text{(by (30))} \\
&\geq \min\{\xi, \zeta\} \sqrt{\mu} n_a(w_j(t_0)) X_{\min}/2,
\end{aligned}$$

which implies that, by the Fundamental Theorem of Calculus,

$$\begin{aligned}
&\cos(w_j(t_0 + \Delta t), x_a(w_j(t_0))) \\
&= \cos(w_j(t_0), x_a(w_j(t_0))) + \int_0^{\Delta t} \frac{d}{dt} \cos(w_j(t_0 + \tau), x_a(w_j(t_0))) d\tau \\
&\geq \cos(w_j(t_0), x_a(w_j(t_0))) + \Delta t \cdot \min\{\xi, \zeta\} \sqrt{\mu} n_a(w_j(t_0)) X_{\min}/2 \\
&= \cos(w_j(t_0), x_a(w_j(t_0))) + 2 \geq 1,
\end{aligned}$$

which leads to  $\cos(w_j(t_0 + \Delta t), x_a(w_j(t_0))) = 1$ . This would imply  $w_j(t_0 + \Delta t) \in \mathcal{S}_+$  because  $x_a(w_j(t_0)) \in \mathcal{S}_+$ , which contradicts our original assumption that  $w_j$  fixes the activation pattern. Therefore,  $\exists 0 < \tau_0 \leq \Delta t$  such that  $\mathbb{1}_{\langle x_i, w_j(t_0 + \tau_0) \rangle > 0} \neq \mathbb{1}_{\langle x_i, w_j(t_0) \rangle > 0}$ , due to the restriction on how  $w_j$  can change its activation pattern, it cannot return to its previous activation pattern, then one must have  $\mathbb{1}_{\langle x_i, w_j(t_0 + \Delta t) \rangle > 0} \neq \mathbb{1}_{\langle x_i, w_j(t_0) \rangle > 0}$ .

- The other case is when  $w_j(t_0) \in \mathcal{S}_-$ . For this case, we need first show that  $w_j(t_0 + \tau) \notin \mathcal{S}_{x_-}^\zeta, \forall 0 \leq \tau \leq \Delta t$ , or more generally,  $\mathcal{S}_{x_-}^\zeta$  does not contain any  $w_j$  in  $\mathcal{V}_+$  during  $[0, T]$ . To see this, let us pick  $x_r = x_-$ , then Lemma 10 suggests that

$$\left| \frac{d}{dt} \psi_{rj} - (\psi_{ra} - \psi_{rj} \psi_{aj}) \|x_a(w_j)\| \right| \leq 2nX_{\max} \max_i |f(x_i; W, v)|.$$

Consider the case when  $\cos(w_j, x_-) = \sqrt{1 - \zeta}$ , i.e.  $w_j$  is at the boundary of  $\mathcal{S}_{x_-}^\zeta$ . We know that in this case,  $w_j \in \mathcal{S}_{x_-}^\zeta \subseteq \mathcal{S}_-$  thus  $x_a(w_j) = -x_-$ , and

$$\left| \frac{d}{dt} \cos(w_j, x_-) \right|_{\cos(w_j, x_-) = \sqrt{1 - \zeta}} + (1 - \cos^2(w_j, x_-)) \|x_-\| \leq 2nX_{\max} \max_i |f(x_i; W, v)|,$$

which is

$$\begin{aligned} & \left| \frac{d}{dt} \cos(w_j, x_-) \right|_{\cos(w_j, x_-) = \sqrt{1 - \zeta}} + \zeta \|x_-\| \leq 2nX_{\max} \max_i |f(x_i; W, v)| \\ \Rightarrow & \frac{d}{dt} \cos(w_j, x_-) \Big|_{\cos(w_j, x_-) = \sqrt{1 - \zeta}} \\ & \leq -\zeta \|x_-\| + 2nX_{\max} \max_i |f(x_i; W, v)| \\ & \leq -\zeta \sqrt{\mu} X_{\min} + 2nX_{\max} \max_i |f(x_i; W, v)| \quad (\text{by Lemma 11}) \\ & \leq -\zeta \sqrt{\mu} X_{\min} / 2 < 0. \quad (\text{by (30)}) \end{aligned}$$

Therefore, during  $[0, T]$ , neuron  $w_j$  in  $\mathcal{V}_+$  cannot enter  $\mathcal{S}_{x_-}^\zeta$  if at initialization,  $w_j(0) \notin \mathcal{S}_{x_-}^\zeta$ , which is guaranteed by (27).

With the argument above, we know that  $w_j(t_0 + \tau) \notin \mathcal{S}_{x_-}^\zeta, \forall 0 \leq \tau \leq \Delta t$ . Again we suppose that  $w_j(t) \in \mathcal{S}_- - \mathcal{S}_{x_-}^\zeta, \forall t \in [t_0, t_0 + \Delta t]$ , i.e.,  $w_j$  fixes its activation during  $[t_0, t_0 + \Delta t]$ . Let us pick  $x_r = x_-$ , then Lemma 10 suggests that

$$\left| \frac{d}{dt} \cos(w_j, x_-) + (1 - \cos^2(w_j, x_-)) \|x_-\| \right| \leq 2nX_{\max} \max_i |f(x_i; W, v)|,$$

which leads to  $\forall t \in [t_0, t_0 + \Delta t]$ ,

$$\begin{aligned} \frac{d}{dt} \cos(w_j, x_-) & \leq -(1 - \cos^2(w_j, x_-)) \|x_-\| + 2nX_{\max} \max_i |f(x_i; W, v)| \\ & \leq -\zeta \|x_-\| + 2nX_{\max} \max_i |f(x_i; W, v)| \quad (w_j \notin \mathcal{S}_{x_-}^\zeta) \\ & \leq -\zeta \sqrt{\mu} n_a(w_j(t_0)) X_{\min} + 2nX_{\max} \max_i |f(x_i; W, v)| \quad (\text{by Lemma 11}) \\ & \leq -\zeta \sqrt{\mu} n_a(w_j(t_0)) X_{\min} / 2. \quad (\text{by (30)}) \\ & \leq -\min\{\xi, \zeta\} \sqrt{\mu} n_a(w_j(t_0)) X_{\min} / 2, \end{aligned}$$

Similarly, by FTC, we have

$$\cos(w_j(t_0 + \Delta t), x_-) \leq -1.$$

This would imply  $w_j(t_0 + \Delta t) \in \mathcal{S}_+$  because  $-x_- = x_a(w_j(t_0)) \in \mathcal{S}_+$ , which contradicts our original assumption that  $w_j$  fixes its activation pattern. Therefore, one must have  $\mathbb{1}_{\langle x_i, w_j(t_0 + \Delta t) \rangle} \neq \mathbb{1}_{\langle x_i, w_j(t_0) \rangle} > 0$ .



In summary, we have shown that, during  $[0, T]$ , a neuron in  $\mathcal{V}_+$  can not keep a fixed activation pattern for a time longer than  $\Delta t = \frac{4}{\min\{\zeta, \xi\} \sqrt{\mu X_{\min}} n_a}$ , where  $n_a$  is the number of data points that activate  $w_j$  under the fixed activation pattern.

**Bound on total travel time until directional convergence** As we have discussed in Section 3.2 and also formally proved here, during alignment phase  $[0, T]$ , a neuron in  $\mathcal{V}_+$  must change its activation pattern within  $\Delta t = \frac{4}{\min\{\zeta, \xi\} \sqrt{\mu X_{\min}} n_a}$  time unless it is in either  $\mathcal{S}_+$  or  $\mathcal{S}_{\text{dead}}$ . And the new activation it is transitioning into must contain no new activation on negative data points and must keep all existing activation on positive data points, together it shows that a neuron must reach either  $\mathcal{S}_+$  or  $\mathcal{S}_{\text{dead}}$  within a fixed amount of time, which is the remaining thing we need to formally show here.

For simplicity of the argument, we first assume  $T = \infty$ , i.e., the alignment phase lasts indefinitely, and we show that a neuron in  $\mathcal{V}_+$  must reach  $\mathcal{S}_+$  or  $\mathcal{S}_{\text{dead}}$  before  $t_1 = \frac{16 \log n}{\min\{\zeta, \xi\} \sqrt{\mu X_{\min}}}$ . Lastly, such directional convergence can be achieved if  $t_1 \leq T$ , which is guaranteed by our choice of  $\epsilon$  in (29).

- For a neuron in  $\mathcal{V}_+$  that reaches  $\mathcal{S}_{\text{dead}}$ , the analysis is easy: It must start with no activation on positive data and then lose activation on negative data one by one until losing all of its activation. Therefore, it must reach  $\mathcal{S}_{\text{dead}}$  before

$$\sum_{k=1}^{n_a(w_j(0))} \frac{4}{\min\{\zeta, \xi\} \sqrt{\mu X_{\min}} k} \leq \frac{4}{\min\{\zeta, \xi\} \sqrt{\mu X_{\min}}} \left( \sum_{k=1}^n \frac{1}{k} \right) \leq \frac{16 \log n}{\min\{\zeta, \xi\} \sqrt{\mu X_{\min}}} = t_1.$$

- For a neuron in  $\mathcal{V}_+$  that reaches  $\mathcal{S}_+$ , there is no difference conceptually, but it can switch its activation pattern in many ways before reaching  $\mathcal{S}_+$ , so it is not straightforward to see its travel time until  $\mathcal{S}_+$  is upper bounded by  $t_1$ .

To formally show the upper bound on the travel time, we need some definition of a path that keeps a record of the activation patterns of a neuron  $w_j(t)$  before it reaches  $\mathcal{S}_+$ .

Let  $n_+ = |\mathcal{I}_+|$ ,  $n_- = |\mathcal{I}_-|$  be the number of positive, negative data respectively, then we call  $\mathcal{P}_{(k^{(0)}, k^{(1)}, \dots, k^{(L)})}$  a *path* of length- $L$ , if

1.  $\forall 0 \leq l \leq L$ , we have  $k^{(l)} = (k_+^{(l)}, k_-^{(l)}) \in \mathbb{N} \times \mathbb{N}$  with  $0 \leq k_+^{(l)} \leq n_+$ ,  $0 \leq k_-^{(l)} \leq n_-$ ;
2. For  $k^{(l_1)}, k^{(l_2)}$  with  $l_1 < l_2$ , we have either  $k_+^{(l_1)} > k_+^{(l_2)}$  or  $k_-^{(l_1)} < k_-^{(l_2)}$ ;
3.  $k^{(L)} = (n_+, 0)$ ;
4.  $k^{(l)} \neq (0, 0), \forall 0 \leq l \leq L$ .

Given all our analysis on how a neuron  $w_j(t)$  can switch its activation pattern in previous parts, we know that for any  $w_j(t)$  that reaches  $\mathcal{S}_+$ , there is an associated  $\mathcal{P}_{(k^{(0)}, k^{(1)}, \dots, k^{(L)})}$  that keeps an ordered record of encountered values of

$$(|\{i \in \mathcal{I}_+ : \langle x_i, w_j(t) \rangle > 0\}|, |\{i \in \mathcal{I}_- : \langle x_i, w_j(t) \rangle > 0\}|),$$

before  $w_j$  reaches  $\mathcal{S}_+$ . That is, a neuron  $w_j$  starts with some activation pattern that activates  $k_+(0)$  positive data and  $k_-(0)$  negative data, then switch its activation pattern (by either losing negative data or gaining positive data) to one that activates  $k_+(1)$  positive data and  $k_-(1)$  negative data. By keep doing so, it reaches  $\mathcal{S}_+$  that activates  $k_+(L) = n_+$  positive data and  $k_-(L) = 0$  negative data. Please see Figure 11 for an illustration of a path.

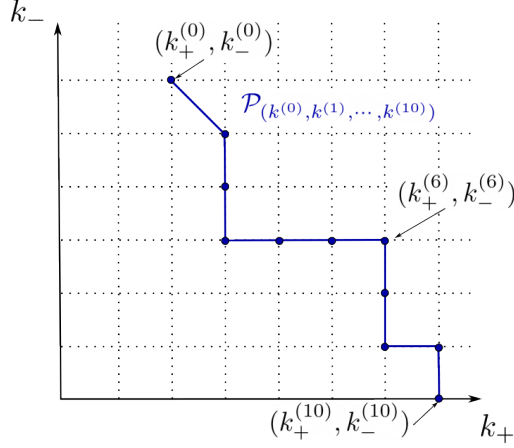


Figure 11: Illustration of a path of length-10. Each dot on the grid represents one  $k^{(l)}$ .

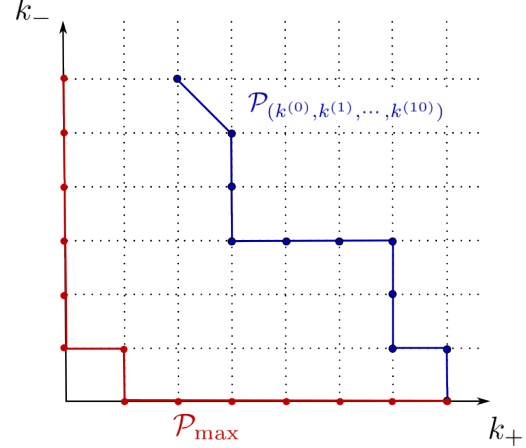


Figure 12: Illustration of a path and the maximal path

Given a path  $\mathcal{P}_{(k^{(0)}, k^{(1)}, \dots, k^{(L)})}$  of neuron  $w_j$ , we define the *travel time* of this path as

$$T(\mathcal{P}_{(k^{(0)}, k^{(1)}, \dots, k^{(L)})}) = \sum_{l=0}^{L-1} \frac{4}{\min\{\zeta, \xi\} \sqrt{\mu} X_{\min}(k_+^{(l)} + k_-^{(l)})},$$

which is exactly the traveling time from  $k^{(0)}$  to  $k^{(L)}$  if one spends  $\frac{4}{\min\{\zeta, \xi\} \sqrt{\mu} X_{\min}(k_+^{(l)} + k_-^{(l)})}$  on the edge between  $k^{(l)}$  and  $k^{(l+1)}$ .

Our analysis shows that if  $w_j$  reaches  $\mathcal{S}_+$ , then

$$\inf\{t : w_j(t) \in \mathcal{S}_+\} \leq T(\mathcal{P}_{(k^{(0)}, k^{(1)}, \dots, k^{(L)})}).$$

Now we define the maximal path  $\mathcal{P}_{\max}$  as a path that has the maximum length  $n = n_+ + n_-$ , which is uniquely determined by the following trajectory of  $k^{(l)}$

$$(0, n_-), (0, n_- - 1), (0, n_- - 2), \dots, (0, 1), (1, 1), (1, 0), \dots, (n_+ - 1, 0), (n_+, 0).$$

Please see Figure 12 for an illustration.

The traveling time for  $\mathcal{P}_{\max}$  is

$$\begin{aligned} T(\mathcal{P}_{\max}) &= \frac{4}{\min\{\zeta, \xi\} \sqrt{\mu} X_{\min}} \left( \sum_{k=1}^{n_-} \frac{1}{k} + \frac{1}{2} + \sum_{k=1}^{n_+ - 1} \frac{1}{k} \right) \\ &\leq \frac{4}{\min\{\zeta, \xi\} \sqrt{\mu} X_{\min}} \left( 2 \sum_{k=1}^n \frac{1}{k} + \frac{1}{2} \right) \\ &\leq \frac{16 \log n}{\min\{\zeta, \xi\} \sqrt{\mu} X_{\min}} = t_1. \end{aligned}$$

The proof is complete by the fact that any path satisfies

$$T(\mathcal{P}_{(k^{(0)}, k^{(1)}, \dots, k^{(L)})}) \leq T(\mathcal{P}_{\max}).$$

This is because there is a one-to-one correspondence between the edges  $(k^{(l)}, k^{(l+1)})$  in  $\mathcal{P}_{(k^{(0)}, k^{(1)}, \dots, k^{(L)})}$  and a subset of edges in  $\mathcal{P}_{\max}$ , and the travel time from of edge  $(k^{(l)}, k^{(l+1)})$  is shorter than the corresponding edge in  $\mathcal{P}_{\max}$ . Formally stating such correspondence is tedious and a visual illustration in Figure 13 and 14 is more effective (Putting all correspondence makes a clustered plot thus we split them into two figures):

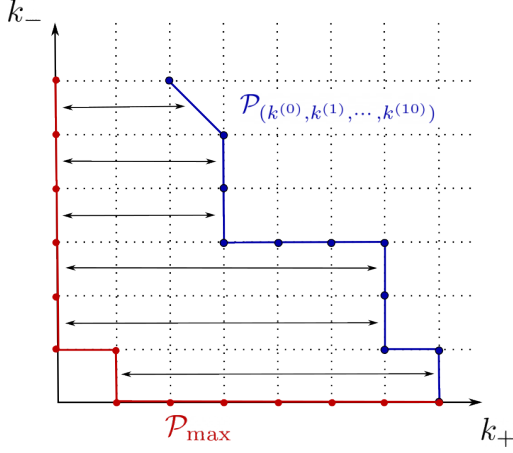


Figure 13: Correspondence between edges in  $\mathcal{P}_{(k^{(0)}, k^{(1)}, \dots, k^{(L)})}$  and  $\mathcal{P}_{\max}$ . (Part 1)

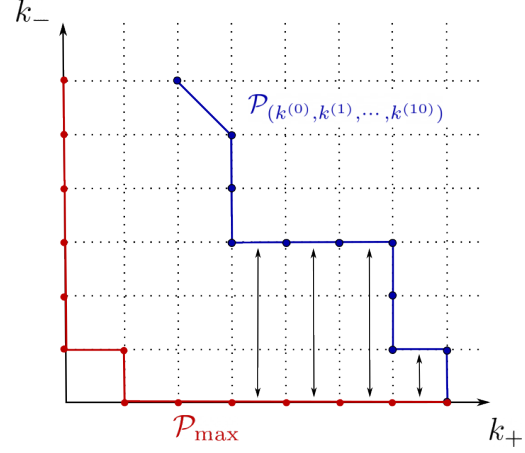


Figure 14: Correspondence between edges in  $\mathcal{P}_{(k^{(0)}, k^{(1)}, \dots, k^{(L)})}$  and  $\mathcal{P}_{\max}$ . (Part 2)

Therefore, if  $w_j$  reaches  $\mathcal{S}_+$ , then it reaches  $\mathcal{S}_+$  within  $t_1$ :

$$\inf\{t : w_j(t) \in \mathcal{S}_+\} \leq T(\mathcal{P}_{(k^{(0)}, k^{(1)}, \dots, k^{(L)})}) \leq T(\mathcal{P}_{\max}) \leq t_1.$$

So far we have shown when the alignment phase lasts long enough, i.e.,  $T$  large enough, the directional convergence is achieved by  $t_1$ . We simply pick  $\epsilon$  such that

$$T = \frac{1}{4nX_{\max}} \log \frac{1}{\sqrt{h\epsilon}} \geq t_1 = \frac{16 \log n}{\min\{\zeta, \xi\} \sqrt{\mu} X_{\min}},$$

and (29) suffices. □

## D Proof for Theorem 1: Final Convergence

Since we have proved the first part of Theorem 1 in Section C, we will use it as a fact, then prove the remaining part of Theorem 1.

### D.1 Auxiliary lemmas

First, we show that  $\mathcal{S}_+$ ,  $\mathcal{S}_-$ ,  $\mathcal{S}_{\text{dead}}$  are trapping regions.

**Lemma 12.** *Consider any solution to the gradient flow dynamic (2), we have the following:*

- If at some time  $t_1 \geq 0$ , we have  $w_j(t_1) \in \mathcal{S}_{\text{dead}}$ , then  $w_j(t_1 + \tau) \in \mathcal{S}_{\text{dead}}$ ,  $\forall \tau \geq 0$ ;
- If at some time  $t_1 \geq 0$ , we have  $w_j(t_1) \in \mathcal{S}_+$  for some  $j \in \mathcal{V}_+$ , then  $w_j(t_1 + \tau) \in \mathcal{S}_+$ ,  $\forall \tau \geq 0$ ;
- If at some time  $t_1 \geq 0$ , we have  $w_j(t_1) \in \mathcal{S}_-$  for some  $j \in \mathcal{V}_-$ , then  $w_j(t_1 + \tau) \in \mathcal{S}_-$ ,  $\forall \tau \geq 0$ ;

*Proof.* The first statement is simple, if  $w_j \in \mathcal{S}_{\text{dead}}$ , then one have  $\dot{w}_j = 0$ , thus  $w_j$  remains in  $\mathcal{S}_{\text{dead}}$ .  
For the second statement, we have, since  $j \in \mathcal{V}_+$ ,

$$\frac{d}{dt}w_j = - \sum_{i=1}^n \mathbb{1}_{\langle x_i, w_j \rangle \geq 0} \nabla_{\hat{y}} \ell(y_i, f(x_i; W, v)) x_i \|w_j\|.$$

By the Fundamental Theorem of Calculus, one writes,  $\forall \tau \geq 0$ ,

$$\begin{aligned} w_j(t_1 + \tau) &= w_j(t_1) + \int_0^\tau \frac{d}{dt}w_j d\tau \\ &= w_j(t_1) + \int_0^\tau - \sum_{i=1}^n \mathbb{1}_{\langle x_i, w_j \rangle \geq 0} \nabla_{\hat{y}} \ell(y_i, f(x_i; W, v)) x_i \|w_j\| d\tau \\ &= w_j(t_1) + \int_0^\tau \sum_{i=1}^n \mathbb{1}_{\langle x_i, w_j \rangle \geq 0} y_i \exp(-y_i f(x_i; W, v)) x_i \|w_j\| d\tau \\ &= w_j(t_1) + \underbrace{\sum_{i \in \mathcal{I}_+} \left( \int_0^\tau \exp(-y_i f(x_i; W, v)) \|w_j\| d\tau \right) x_i}_{:= \tilde{x}_+}. \end{aligned}$$

Here  $w_j(t_1) \in \mathcal{S}_+$  by our assumption,  $\tilde{x}_+ \in K \subseteq \mathcal{S}_+$  because  $\tilde{x}_+$  is a conical combination of  $x_i, i \in \mathcal{I}_+$ . Since  $\mathcal{S}_+$  is a convex cone, we have  $w_j(t_1 + \tau) \in \mathcal{S}_+$  as well.

The proof of the third statement is almost identical: when  $j \in \mathcal{V}_-$ , we have

$$\frac{d}{dt}w_j = \sum_{i=1}^n \mathbb{1}_{\langle x_i, w_j \rangle \geq 0} \nabla_{\hat{y}} \ell(y_i, f(x_i; W, v)) x_i \|w_j\|,$$

and

$$w_j(t_1 + \tau) = w_j(t_1) + \underbrace{\sum_{i \in \mathcal{I}_-} \left( \int_0^\tau \exp(-y_i f(x_i; W, v)) \|w_j\| d\tau \right) x_i}_{:= \tilde{x}_-}.$$

Again, here  $w_j(t_1) \in \mathcal{S}_-$  by our assumption,  $\tilde{x}_- \in -K \subseteq \mathcal{S}_-$  because  $\tilde{x}_-$  is a conical combination of  $x_i, i \in \mathcal{I}_-$ . Since  $\mathcal{S}_-$  is a convex cone, we have  $w_j(t_1 + \tau) \in \mathcal{S}_-$  as well.  $\square$

Then the following Lemma provides a lower bound on neuron norms upon  $t_1$ .

**Lemma 13.** *Consider any solution to the gradient flow dynamic (2) starting from initialization (3). Let  $t_1$  be the time when directional convergence is achieved, as defined in Theorem 1, and we define  $\tilde{\mathcal{V}}_+ : \{j : w_j(t_1) \in \mathcal{S}_+\}$  and  $\tilde{\mathcal{V}}_- : \{j : w_j(t_1) \in \mathcal{S}_-\}$ . If both  $\tilde{\mathcal{V}}_+$  and  $\tilde{\mathcal{V}}_-$  are non-empty, we have*

$$\begin{aligned} \sum_{j \in \tilde{\mathcal{V}}_+} \|w_j(t_1)\|^2 &\geq \exp(-4nX_{\max}t_1) \sum_{j \in \tilde{\mathcal{V}}_+} \|w_j(0)\|^2, \\ \sum_{j \in \tilde{\mathcal{V}}_-} \|w_j(t_1)\|^2 &\geq \exp(-4nX_{\max}t_1) \sum_{j \in \tilde{\mathcal{V}}_-} \|w_j(0)\|^2, \end{aligned}$$

*Proof.* We have shown that

$$\frac{d}{dt} \|w_j\|^2 = -2 \sum_{i=1}^n \mathbb{1}_{\langle x_i, w_j \rangle \geq 0} \nabla_{\hat{y}} \ell(y_i, f(x_i; W, v)) \langle x_i, w_j \rangle \text{sign}(v_j(0)) \|w_j\|.$$

Then before  $t_1$ , we have  $\forall j \in [h]$

$$\begin{aligned} \frac{d}{dt} \|w_j\|^2 &= -2 \sum_{i=1}^n \mathbb{1}_{\langle x_i, w_j \rangle \geq 0} \nabla_{\hat{y}} \ell(y_i, f(x_i; W, v)) \langle x_i, w_j \rangle \text{sign}(v_j(0)) \|w_j\| \\ &\geq -2 \sum_{i=1}^n (|y_i| + 2 \max_i |f(x_i; W, v)|) \|x_i\| \|w_j\|^2 \\ &\geq -4 \sum_{i=1}^n \|x_i\| \|w_j\|^2 \geq -4nX_{\max} \|w_j\|^2, \end{aligned}$$

where the second last inequality is because  $\max_i |f(x_i; W, v)| \leq \frac{1}{2}$  before  $t_1$ . Summing over  $j \in \tilde{\mathcal{V}}_+$ , we have

$$\frac{d}{dt} \sum_{j \in \tilde{\mathcal{V}}_+} \|w_j\|^2 \geq -4nX_{\max} \sum_{j \in \tilde{\mathcal{V}}_+} \|w_j\|^2.$$

Therefore, we have the following bound:

$$\sum_{j \in \tilde{\mathcal{V}}_+} \|w_j(t_1)\|^2 \geq \exp(-4nX_{\max}t_1) \sum_{j \in \tilde{\mathcal{V}}_+} \|w_j(0)\|^2.$$

□

Moreover, after  $t_1$ , the neuron norms are non-decreasing, as suggested by

**Lemma 14.** *Consider any solution to the gradient flow dynamic (2) starting from initialization (3). Let  $t_1$  be the time when directional convergence is achieved, as defined in Theorem 1, and we define  $\tilde{\mathcal{V}}_+ : \{j : w_j(t_1) \in \mathcal{S}_+\}$  and  $\tilde{\mathcal{V}}_- : \{j : w_j(t_1) \in \mathcal{S}_-\}$ . If both  $\tilde{\mathcal{V}}_+$  and  $\tilde{\mathcal{V}}_-$  are non-empty, we have  $\forall \tau \geq 0$  and  $t_2 \geq t_1$ ,*

$$\sum_{j \in \tilde{\mathcal{V}}_+} \|w_j(t_2 + \tau)\|^2 \geq \sum_{j \in \tilde{\mathcal{V}}_+} \|w_j(t_2)\|^2, \quad \sum_{j \in \tilde{\mathcal{V}}_-} \|w_j(t_2 + \tau)\|^2 \geq \sum_{j \in \tilde{\mathcal{V}}_-} \|w_j(t_2)\|^2 \quad (31)$$

*Proof.* It suffices to show that after  $t_1$ , the following derivatives:

$$\frac{d}{dt} \sum_{j \in \tilde{\mathcal{V}}_+} \|w_j(t)\|^2, \quad \frac{d}{dt} \sum_{j \in \tilde{\mathcal{V}}_-} \|w_j(t)\|^2,$$

are non-negative.

For  $j \in \tilde{\mathcal{V}}_+$ ,  $w_j$  stays in  $\mathcal{S}_+$  by Lemma 12, and we have

$$\begin{aligned} \frac{d}{dt} \|w_j\|^2 &= -2 \sum_{i \in \mathcal{I}_+} \nabla_{y_i} \ell(y_i, f(x_i; W, v)) \langle x_i, w_j \rangle \|w_j\|. \\ &= 2 \sum_{i \in \mathcal{I}_+} y_i \ell(y_i, f(x_i; W, v)) \langle x_i, w_j \rangle \|w_j\| \geq 0. \end{aligned}$$

Summing over  $j \in \tilde{\mathcal{V}}_+$ , we have  $\frac{d}{dt} \sum_{j \in \tilde{\mathcal{V}}_+} \|w_j(t)\|^2 \geq 0$ . Similarly one has  $\frac{d}{dt} \sum_{j \in \tilde{\mathcal{V}}_-} \|w_j(t)\|^2 \geq 0$ .  $\square$

Finally, the following lemma is used for deriving the final convergence.

**Lemma 15.** *Consider the following loss function*

$$\mathcal{L}_{lin}(W, v) = \sum_{i=1}^n \ell(y_i, v^\top W^\top x_i),$$

if  $\{x_i, y_i\}, i \in [n]$  are linearly separable, i.e.,  $\exists \gamma > 0$  and  $z \in \mathbb{S}^{D-1}$  such that  $y_i \langle z, x_i \rangle \geq \gamma, \forall i \in [n]$ , then under the gradient flow on  $\mathcal{L}_{lin}(W, v)$ , we have

$$\dot{\mathcal{L}}_{lin} \leq -\|v\|^2 \mathcal{L}^2 \gamma^2. \quad (32)$$

*Proof.*

$$\begin{aligned} \dot{\mathcal{L}} &= -\|\nabla_W \mathcal{L}\|_F^2 - \|\nabla_v \mathcal{L}\|_F^2 \leq -\|\nabla_W \mathcal{L}\|_F^2 \\ &= -\left\| \sum_{i=1}^n y_i \ell(y_i, v^\top W^\top x_i) x_i v^\top \right\|_F^2 \\ &= -\|v\|^2 \left\| \sum_{i=1}^n y_i \ell(y_i, v^\top W^\top x_i) x_i \right\|^2 \\ &\leq -\|v\|^2 \left| \left\langle z, \sum_{i=1}^n y_i \ell(y_i, v^\top W^\top x_i) x_i \right\rangle \right|^2 \\ &\leq -\|v\|^2 \left| \sum_{i=1}^n \ell(y_i, v^\top W^\top x_i) \gamma \right|^2 \leq -\|v\|^2 \mathcal{L}^2 \gamma^2. \end{aligned}$$

$\square$

## D.2 Proof of final convergence

*Proof of Theorem 1: Second Part.* By Lemma 12, we know that after  $t_1$ , neurons in  $S_+$  ( $S_-$ ) stays in  $S_+$  ( $S_-$ ). Thus the loss can be decomposed as

$$\mathcal{L} = \underbrace{\sum_{i \in \mathcal{I}_+} \ell \left( y_i, \sum_{j \in \tilde{\mathcal{V}}_+} v_j \langle w_j, x_i \rangle \right)}_{\mathcal{L}_+} + \underbrace{\sum_{i \in \mathcal{I}_-} \ell \left( y_i, \sum_{j \in \tilde{\mathcal{V}}_-} v_j \langle w_j, x_i \rangle \right)}_{\mathcal{L}_-}, \quad (33)$$

where  $\tilde{\mathcal{V}}_+ : \{j : w_j(t_1) \in S_+\}$  and  $\tilde{\mathcal{V}}_- : \{j : w_j(t_1) \in S_-\}$ . Therefore, the training after  $t_1$  is decoupled into 1) using neurons in  $\tilde{\mathcal{V}}_+$  to fit positive data in  $\mathcal{I}_+$  and 2) using neurons in  $\tilde{\mathcal{V}}_-$  to fit positive data in  $\mathcal{I}_-$ .

We define  $f_+(x_i; W, v) = \sum_{j \in \tilde{\mathcal{V}}_+} v_j \langle w_j, x_i \rangle$  and let  $t_2^+ = \inf\{t : \max_{i \in \mathcal{I}_+} |f_+(x_i; W, v)| > \frac{1}{4}\}$ . Similarly, we also define  $f_-(x_i; W, v) = \sum_{j \in \tilde{\mathcal{V}}_-} v_j \langle w_j, x_i \rangle$  and let  $t_2^- = \inf\{t : \max_{i \in \mathcal{I}_-} |f_-(x_i; W, v)| > \frac{1}{4}\}$ . Then  $t_1 \leq \min\{t_2^+, t_2^-\}$ , by Lemma 3.

$\mathcal{O}(1/t)$  **convergence after  $t_2$** : We first show that when both  $t_2^+, t_2^-$  are finite, then it implies  $\mathcal{O}(1/t)$  convergence on the loss. Then we show that they are indeed finite and  $t_2 := \max\{t_2^+, t_2^-\} = \mathcal{O}(\frac{1}{n} \log \frac{1}{\epsilon})$ .

At  $t_2 = \max\{t_2^+, t_2^-\}$ , by definition,  $\exists i_+ \in \mathcal{I}_+$  such that

$$\frac{1}{4} \leq f_+(x_{i_+}; W, v) \leq \sum_{j \in \tilde{\mathcal{V}}_+} v_j \langle w_j, x_{i_+} \rangle \leq \sum_{j \in \tilde{\mathcal{V}}_+} \|w_j\|^2 \|x_{i_+}\|, \quad (34)$$

which implies, by Lemma 14,  $\forall t \geq t_2$

$$\sum_{j \in \tilde{\mathcal{V}}_+} \|w_j(t)\|^2 \geq \sum_{j \in \tilde{\mathcal{V}}_+} \|w_j(t_2)\|^2 \geq \frac{1}{4\|x_{i_+}\|} \geq \frac{1}{4X_{\max}}. \quad (35)$$

Similarly, we have  $\forall t \geq t_2$ ,

$$\sum_{j \in \tilde{\mathcal{V}}_-} \|w_j(t)\|^2 \geq \frac{1}{4X_{\max}}. \quad (36)$$

Under the gradient flow dynamics (2), we apply Lemma 15 to the decomposed loss (33)

$$\dot{\mathcal{L}} \leq - \left( \sum_{j \in \tilde{\mathcal{V}}_+} v_j^2 \right) \cdot \mathcal{L}_+^2 \cdot (\mu X_{\min})^2 - \left( \sum_{j \in \tilde{\mathcal{V}}_-} v_j^2 \right) \cdot \mathcal{L}_-^2 \cdot (\mu X_{\min})^2.$$

Here, we can pick the same  $\gamma = \mu X_{\min}$  for both  $\mathcal{L}_+$  and  $\mathcal{L}_-$  because  $\{x_i, y_i\}, i \in \mathcal{I}_+$  is linearly separable with  $z = \frac{y_1 x_1}{\|x_1\|} : \langle z, x_i y_i \rangle \geq \mu \|x_i\| \geq \mu X_{\min}$  by Assumption 1. And similarly,  $\{x_i, y_i\}, i \in \mathcal{I}_-$  is linearly separable with  $\langle z, x_i y_i \rangle \geq \mu \|x_i\| \geq \mu X_{\min}$ . Replace  $v_i^2$  by  $\|w_j\|^2$  from balancedness, together with (35)(36), we have

$$\begin{aligned} \dot{\mathcal{L}} &\leq - \left( \sum_{j \in \tilde{\mathcal{V}}_+} \|w_j\|^2 \right) \cdot \mathcal{L}_+^2 \cdot (\mu X_{\min})^2 - \left( \sum_{j \in \tilde{\mathcal{V}}_-} \|w_j\|^2 \right) \cdot \mathcal{L}_-^2 \cdot (\mu X_{\min})^2 \\ &\leq - \frac{(\mu X_{\min})^2}{4X_{\max}} (\mathcal{L}_+^2 + \mathcal{L}_-^2) \leq - \frac{(\mu X_{\min})^2}{8X_{\max}} (\mathcal{L}_+ + \mathcal{L}_-)^2 = - \frac{(\mu X_{\min})^2}{8X_{\max}} \mathcal{L}^2, \end{aligned}$$

which is

$$\frac{1}{\mathcal{L}^2} \dot{\mathcal{L}} \leq -\frac{(\mu X_{\min})^2}{8X_{\max}}.$$

Integrating both side from  $t_2$  to any  $t \geq t_2$ , we have

$$\frac{1}{\mathcal{L}} \Big|_{t_2}^t \leq -\frac{(\mu X_{\min})^2}{8X_{\max}}(t - t_2),$$

which leads to

$$\mathcal{L}(t) \leq \frac{\mathcal{L}(t_2)}{\mathcal{L}(t_2)\alpha(t - t_2) + 1}, \text{ where } \alpha = \frac{(\mu X_{\min})^2}{8X_{\max}}.$$

**Showing  $t_2 = \mathcal{O}(\frac{1}{n} \log \frac{1}{\epsilon})$ :** The remaining thing is to show  $t_2$  is  $\mathcal{O}(\frac{1}{n} \log \frac{1}{\epsilon})$ .

Since after  $t_1$ , the gradient dynamics are fully decoupled into two gradient flow dynamics (on  $\mathcal{L}_+$  and on  $\mathcal{L}_-$ ), it suffices to show  $t_2^+ = \mathcal{O}(\frac{1}{n} \log \frac{1}{\epsilon})$  and  $t_2^- = \mathcal{O}(\frac{1}{n} \log \frac{1}{\epsilon})$  separately, then combine them to show  $t_2 = \max\{t_2^+, t_2^-\} = \mathcal{O}(\frac{1}{n} \log \frac{1}{\epsilon})$ . The proof is almost identical for  $\mathcal{L}_+$  and  $\mathcal{L}_-$ , thus we only prove  $t_2^+ = \mathcal{O}(\frac{1}{n} \log \frac{1}{\epsilon})$  here.

Suppose

$$t_2 \geq t_1 + \frac{6}{\sqrt{\mu}n_+X_{\min}} + \frac{4}{\sqrt{\mu}n_+X_{\min}} \left( \log \frac{2}{\epsilon^2 \sqrt{\mu}X_{\min}W_{\min}^2} + 4nX_{\max}t_1 \right), \quad (37)$$

where  $n_+ = |\mathcal{I}_+|$ . It takes two steps to show a contradiction: First, we show that for some  $t_a \geq 0$ , a refined alignment  $\cos(w_j(t_1 + t_a), x_+) \geq \frac{1}{4}, \forall j \in \tilde{\mathcal{V}}_+$  is achieved, and such refined alignment is maintained until at least  $t_2^+$ :  $\cos(w_j(t), x_+) \geq \frac{1}{4}, \forall j \in \tilde{\mathcal{V}}_+$  for all  $t_1 + t_a \leq t \leq t_2^+$ . Then, keeping this refined alignment leads to a contradiction.

- For  $j \in \tilde{\mathcal{V}}_+$ , we have

$$\frac{d}{dt} \frac{w_j}{\|w_j\|} = \left( I - \frac{w_j w_j^\top}{\|w_j\|^2} \right) \underbrace{\left( \sum_{i \in \mathcal{I}_+} -\nabla_{\hat{y}} \ell(y_i, f_+(x_i; W, v)) x_i \right)}_{:= \tilde{x}_a}.$$

Then

$$\begin{aligned} \frac{d}{dt} \cos(x_+, w_j) &= (\cos(x_+, \tilde{x}_a) - \cos(x_+, w_j) \cos(\tilde{x}_a, w_j)) \|\tilde{x}_a\| \\ &\geq (\cos(x_+, \tilde{x}_a) - \cos(x_+, w_j)) \|\tilde{x}_a\|. \end{aligned}$$

We can show that  $\cos(x_+, \tilde{x}_a) \geq \frac{1}{3}$  and  $\|\tilde{x}_a\| \geq \sqrt{\mu}n_+X_{\min}/2$  when  $t_1 \leq t \leq t_2^+$  (we defer the proof to the end as it breaks the flow), thus within  $[t_1, t_2^+]$ , we have

$$\frac{d}{dt} \cos(x_+, w_j) \geq \left( \frac{1}{3} - \cos(x_+, w_j) \right) \sqrt{\mu}n_+X_{\min}/2. \quad (38)$$

We use (38) in two ways: First, since

$$\frac{d}{dt} \cos(x_+, w_j) \Big|_{\cos(x_+, w_j) = \frac{1}{4}} \geq \frac{\sqrt{\mu}n_+X_{\min}}{24} > 0,$$



$\cos(x_+, w_j) \geq \frac{1}{4}$  is a trapping region for  $w_j$  during  $[t_1, t_2^+]$ . Define  $t_a := \inf\{t \geq t_1 : \min_{j \in \tilde{\mathcal{V}}_+} \cos(x_+, w_j(t)) \geq \frac{1}{4}\}$ , then clearly, if  $t_a \leq t_2^+$ , then  $\cos(w_j(t), x_+) \geq \frac{1}{4}, \forall j \in \tilde{\mathcal{V}}_+$  for all  $t_1 + t_a \leq t \leq t_2^+$ .

Now we use (38) again to show that  $t_a \leq t_1 + \frac{6}{\sqrt{\mu}n_+X_{\min}}$ : Suppose that  $t_a \geq t_1 + \frac{6}{\sqrt{\mu}n_+X_{\min}}$ , then  $\exists j^*$  such that  $\cos(x_+, w_{j^*}(t)) < \frac{1}{4}, \forall t \in [t_1, t_1 + \frac{6}{\sqrt{\mu}n_+X_{\min}}]$ , and we have

$$\frac{d}{dt} \cos(x_+, w_{j^*}) \geq \left( \frac{1}{3} - \cos(x_+, w_{j^*}) \right) \sqrt{\mu}n_+X_{\min}/2 \geq \frac{\sqrt{\mu}n_+X_{\min}}{24}. \quad (39)$$

This shows

$$\cos(x_+, w_{j^*}(t_1 + 1)) \geq \cos(x_+, w_{j^*}(t_1)) + \frac{1}{4} \geq \frac{1}{4},$$

which contradicts that  $\cos(x_+, w_{j^*}(t)) < \frac{1}{4}$ . Hence we know  $t_a \leq t_1 + \frac{6}{\sqrt{\mu}n_+X_{\min}}$ .

In summary, we have  $\cos(w_j(t), x_+) \geq \frac{1}{4}, \forall j \in \tilde{\mathcal{V}}_+$  for all  $t_1 + \frac{6}{\sqrt{\mu}n_+X_{\min}} \leq t \leq t_2^+$ .

- Now we check the dynamics of  $\sum_{j \in \tilde{\mathcal{V}}_+} \|w_j(t)\|^2$  during  $t_1 + \frac{6}{\sqrt{\mu}n_+X_{\min}} \leq t \leq t_2^+$ . For simplicity, we denote  $t_1 + \frac{6}{\sqrt{\mu}n_+X_{\min}} := t'_1$ .

For  $j \in \tilde{\mathcal{V}}_+$ , we have, for  $t'_1 \leq t \leq t_2^+$ ,

$$\begin{aligned} \frac{d}{dt} \|w_j\|^2 &= 2 \sum_{i \in \mathcal{I}_+} -\nabla_{y_i} \ell(y_i, f(x_i; W, v)) \langle x_i, w_j \rangle \|w_j\| \\ &\geq \sum_{i \in \mathcal{I}_+} \langle x_i, w_j \rangle \|w_j\| && \text{(by (41))} \\ &= \langle x_+, w_j \rangle \|w_j\| \\ &= \|x_+\| \|w_j\|^2 \cos(x_+, w_j) \\ &\geq \frac{1}{4} \|x_+\| \|w_j\|^2 && \text{(Since } t \geq t'_1\text{)} \\ &\geq \frac{\sqrt{\mu}n_+X_{\min}}{4} \|w_j\|^2, && \text{(by Lemma 11)} \end{aligned}$$

which leads to (summing over  $j \in \tilde{\mathcal{V}}_+$ )

$$\frac{d}{dt} \sum_{j \in \tilde{\mathcal{V}}_+} \|w_j\|^2 \geq \frac{\sqrt{\mu}n_+X_{\min}}{4} \sum_{j \in \tilde{\mathcal{V}}_+} \|w_j\|^2.$$

By Gronwall's inequality, we have

$$\begin{aligned}
& \sum_{j \in \tilde{\mathcal{V}}_+} \|w_j(t_2^+)\|^2 \\
& \geq \exp\left(\frac{\sqrt{\mu}n_+ X_{\min}}{4}(t_2^+ - t_1^+)\right) \sum_{j \in \tilde{\mathcal{V}}_+} \|w_j(t_1^+)\|^2 \\
& \geq \exp\left(\frac{\sqrt{\mu}n_+ X_{\min}}{4}(t_2^+ - t_1^+)\right) \sum_{j \in \tilde{\mathcal{V}}_+} \|w_j(t_1)\|^2 && \text{(By Lemma 14)} \\
& \geq \exp\left(\frac{\sqrt{\mu}n_+ X_{\min}}{4}(t_2^+ - t_1^+)\right) \exp(-4nX_{\max}t_1) \sum_{j \in \tilde{\mathcal{V}}_+} \|w_j(0)\|^2 && \text{(By Lemma 13)} \\
& \geq \exp\left(\frac{\sqrt{\mu}n_+ X_{\min}}{4}(t_2^+ - t_1^+)\right) \exp(-4nX_{\max}t_1) \epsilon^2 W_{\min}^2 \geq \frac{2}{\sqrt{\mu}X_{\min}}. && \text{(by (37))}
\end{aligned}$$

However, at  $t_2^+$ , we have

$$\begin{aligned}
\frac{1}{4} & \geq \frac{1}{n_+} \sum_{i \in \mathcal{I}_+} f_+(x_i; W, v) = \frac{1}{n_+} \sum_{i \in \mathcal{I}_+} \sum_{j \in \tilde{\mathcal{V}}_+} v_j \langle w_j, x_i \rangle \\
& = \frac{1}{n_+} \sum_{j \in \tilde{\mathcal{V}}_+} v_j \langle w_j, x_+ \rangle * \\
& = \frac{1}{n_+} \sum_{j \in \tilde{\mathcal{V}}_+} \|w_j\|^2 \cos(w_j, x_+) \|x_+\| \\
& \geq \frac{1}{4n_+} \sum_{j \in \tilde{\mathcal{V}}_+} \|w_j\|^2 \|x_+\| && \text{(Since } t \geq t_1^+) \\
& \geq \frac{1}{4} \sum_{j \in \tilde{\mathcal{V}}_+} \|w_j\|^2 \sqrt{\mu}X_{\min}, && \text{(by Lemma 11)}
\end{aligned}$$

which suggests  $\sum_{j \in \tilde{\mathcal{V}}_+} \|w_j\|^2 \leq \frac{1}{\sqrt{\mu}X_{\min}}$ . A contradiction.

Therefore, we must have

$$t_2^+ \leq t_1 + \frac{6}{\sqrt{\mu}n_+ X_{\min}} + \frac{4}{\sqrt{\mu}n_+ X_{\min}} \left( \log \frac{2}{\epsilon^2 \sqrt{\mu}X_{\min} W_{\min}^2} + 4nX_{\max}t_1 \right). \quad (40)$$

Since the dominant term here is  $\frac{4}{\sqrt{\mu}n_+ X_{\min}} \log \frac{2}{\epsilon^2 \sqrt{\mu}X_{\min} W_{\min}^2}$ , we have  $t_2^+ = \mathcal{O}(\frac{1}{n} \log \frac{1}{\epsilon})$ . A similar analysis shows  $t_2^- = \mathcal{O}(\frac{1}{n} \log \frac{1}{\epsilon})$ . Therefore  $t_2 = \max\{t_2^+, t_2^-\} = \mathcal{O}(\frac{1}{n} \log \frac{1}{\epsilon})$

**Complete the missing pieces** We have two claims remaining to be proved. The first is  $\cos(x_+, \tilde{x}_a) \geq \frac{1}{2}$  when  $t_1 \leq t \leq t_2^+$ . Since  $x_+ = \sum_{i \in \mathcal{I}_+} x_i$  and  $\tilde{x}_a = \sum_{i \in \mathcal{I}_+} -\nabla_{\hat{y}} \ell(y_i, f_+(x_i; W, v)) x_i$ . We simply use the fact that before  $t_2^+$ , we have, by Lemma 2,

$$\frac{1}{2} \leq -\nabla_{\hat{y}} \ell(y_i, f_+(x_i; W, v)) \leq \frac{3}{2}, \quad (41)$$

to show the following

$$\begin{aligned}
\cos(x_+, \tilde{x}_a) &= \frac{\langle x_+, \tilde{x}_a \rangle}{\|x_+\| \|\tilde{x}_a\|} \\
&= \frac{\sum_{i,j \in \mathcal{I}_+} (-\nabla_{\hat{y}} \ell(y_i, f_+(x_i; W, v))) \langle x_i, x_j \rangle}{\sqrt{\sum_{i,j \in \mathcal{I}_+} \langle x_i, x_j \rangle} \sqrt{\sum_{i,j \in \mathcal{I}_+} (-\nabla_{\hat{y}} \ell(y_i, f_+(x_i; W, v)))^2 \langle x_i, x_j \rangle}} \\
&\geq \frac{\frac{1}{2} \sum_{i,j \in \mathcal{I}_+} \langle x_i, x_j \rangle}{\sqrt{\sum_{i,j \in \mathcal{I}_+} \langle x_i, x_j \rangle} \sqrt{\sum_{i,j \in \mathcal{I}_+} (-\nabla_{\hat{y}} \ell(y_i, f_+(x_i; W, v)))^2 \langle x_i, x_j \rangle}} \\
&\geq \frac{\frac{1}{2} \sum_{i,j \in \mathcal{I}_+} \langle x_i, x_j \rangle}{\sqrt{\sum_{i,j \in \mathcal{I}_+} \langle x_i, x_j \rangle} \sqrt{\sum_{i,j \in \mathcal{I}_+} (\frac{3}{2})^2 \langle x_i, x_j \rangle}} \geq \frac{1}{3},
\end{aligned}$$

since all  $\langle x_i, x_j \rangle, i, j \in \mathcal{I}_+$  are non-negative.

The second claim is  $\|\tilde{x}_a\| \geq \sqrt{\mu n_+ X_{\min}}/2$  is due to that

$$\|\tilde{x}_a\| = \sqrt{\sum_{i,j \in \mathcal{I}_+} (-\nabla_{\hat{y}} \ell(y_i, f_+(x_i; W, v)))^2 \langle x_i, x_j \rangle} \geq \frac{1}{2} \sqrt{\sum_{i,j \in \mathcal{I}_+} \langle x_i, x_j \rangle} = \frac{\|x_+\|}{2} \geq \frac{\sqrt{\mu n_+ X_{\min}}}{2},$$

where the last inequality is from Lemma 11. □

### D.3 Proof of low-rank bias

So far we have proved the directional convergence at the early alignment phase and final  $\mathcal{O}(1/t)$  convergence of the loss in the later stage. The only thing that remains to be shown is the low-rank bias. The proof is quite straightforward but we need some additional notations.

As we proved above, after  $t_1$ , neurons in  $\mathcal{S}_+$  ( $\mathcal{S}_-$ ) stays in  $\mathcal{S}_+$  ( $\mathcal{S}_-$ ). Thus the loss can be decomposed as

$$\mathcal{L} = \underbrace{\sum_{i \in \mathcal{I}_+} \ell \left( y_i, \sum_{j \in \tilde{\mathcal{V}}_+} v_j \langle w_j, x_i \rangle \right)}_{\mathcal{L}_+} + \underbrace{\sum_{i \in \mathcal{I}_-} \ell \left( y_i, \sum_{j \in \tilde{\mathcal{V}}_-} v_j \langle w_j, x_i \rangle \right)}_{\mathcal{L}_-},$$

where  $\tilde{\mathcal{V}}_+ : \{j : w_j(t_1) \in \mathcal{S}_+\}$  and  $\tilde{\mathcal{V}}_- : \{j : w_j(t_1) \in \mathcal{S}_-\}$ . Therefore, the training after  $t_1$  is decoupled into 1) using neurons in  $\tilde{\mathcal{V}}_+$  to fit positive data in  $\mathcal{I}_+$  and 2) using neurons in  $\tilde{\mathcal{V}}_-$  to fit positive data in  $\mathcal{I}_-$ . We use

$$W_+ = [W]_{:, \tilde{\mathcal{V}}_+}, \quad W_- = [W]_{:, \tilde{\mathcal{V}}_-}$$

to denote submatrices of  $W$  by picking only columns in  $\tilde{\mathcal{V}}_+$  and  $\tilde{\mathcal{V}}_-$ , respectively. Similarly, we define

$$v_+ = [v]_{\tilde{\mathcal{V}}_+}, \quad v_- = [v]_{\tilde{\mathcal{V}}_-}$$

for the second layer weight  $v$ . Lastly, we also define

$$W_{\text{dead}} = [W]_{:, \tilde{\mathcal{V}}_{\text{dead}}}, \quad v_{\text{dead}} = [v]_{\tilde{\mathcal{V}}_{\text{dead}}},$$

where  $\tilde{\mathcal{V}}_{\text{dead}} := \{j : w_j(t_1) \in \mathcal{S}_{\text{dead}}\}$ . Given these notations, after  $t_1$  the loss is decomposed as

$$\mathcal{L} = \underbrace{\sum_{i \in \mathcal{I}_+} \ell(y_i, x_i^\top W_+ v_+)}_{\mathcal{L}_+} + \underbrace{\sum_{i \in \mathcal{I}_-} \ell(y_i, x_i^\top W_- v_-)}_{\mathcal{L}_-},$$

and the GF on  $\mathcal{L}$  is equivalent to GF on  $\mathcal{L}_+$  and  $\mathcal{L}_-$  separately. It suffices to study one of them. For GF on  $\mathcal{L}_+$ , we have the following important invariance [23]  $\forall t \geq t_1$ :

$$W_+^\top(t)W_+(t) - v_+(t)v_+^\top(t) = W_+^\top(t_1)W_+(t_1) - v_+(t_1)v_+^\top(t_1),$$

from which one has

$$\begin{aligned} \|W_+^\top(t)W_+(t) - v_+(t)v_+^\top(t)\|_2 &= \|W_+^\top(t_1)W_+(t_1) - v_+(t_1)v_+^\top(t_1)\|_2 \\ &\leq \|W_+^\top(t_1)W_+(t_1)\|_2 - \|v_+(t_1)v_+^\top(t_1)\|_2 \\ &\leq \text{tr}(W_+^\top(t_1)W_+(t_1)) + \|v_+(t_1)\|^2 \\ &= 2 \sum_{j \in \tilde{\mathcal{V}}_+} \|w_j(t_1)\|^2 \leq \frac{4\epsilon W_{\max}^2}{\sqrt{h}} |\tilde{\mathcal{V}}_+|, \end{aligned}$$

where the last inequality is by Lemma 3. Then one can immediately get

$$\|v_+(t)v_+^\top(t)\|_2 - \|W_+^\top(t)W_+(t)\|_2 \leq \|W_+^\top(t)W_+(t) - v_+(t)v_+^\top(t)\|_2 \leq \frac{4\epsilon W_{\max}^2}{\sqrt{h}} |\tilde{\mathcal{V}}_+|,$$

which is precisely

$$\|W_+(t)\|_F^2 \leq \|W_+(t)\|_2^2 + \frac{4\epsilon W_{\max}^2}{\sqrt{h}} |\tilde{\mathcal{V}}_+|. \quad (42)$$

Similarly, we have

$$\|W_-(t)\|_F^2 \leq \|W_-(t)\|_2^2 + \frac{4\epsilon W_{\max}^2}{\sqrt{h}} |\tilde{\mathcal{V}}_-|. \quad (43)$$

Lastly, one has

$$\|W_{\text{dead}}\|_F^2 = \sum_{j \in \tilde{\mathcal{V}}_{\text{dead}}} \|w_j(t_1)\|^2 \leq \frac{4\epsilon W_{\max}^2}{\sqrt{h}} |\tilde{\mathcal{V}}_{\text{dead}}| \quad (44)$$

Adding (42)(43)(44) together, we have

$$\begin{aligned} \|W(t)\|_F^2 &= \|W_+(t)\|_F^2 + \|W_-(t)\|_F^2 + \|W_{\text{dead}}\|_F^2 \\ &\leq \|W_+(t)\|_2^2 + \|W_-(t)\|_2^2 + \frac{4\sqrt{h}\epsilon W_{\max}^2}{\sqrt{h}} \leq 2\|W(t)\|_2^2 + 4\sqrt{h}\epsilon W_{\max}^2. \end{aligned}$$

Finally, since we have shown  $\mathcal{L} \rightarrow 0$  as  $t \rightarrow \infty$ , then  $\forall i \in [n]$ , we have  $\ell(y_i, f(x_i; W, v)) \rightarrow 0$ . This implies

$$f(x_i; W, v) = -\frac{1}{y_i} \log \ell(y_i, f(x_i; W, v)) \rightarrow \infty.$$

Because we have shown that

$$f(x_i; W, v) \leq \sum_{j \in [h]} \|w_j\|^2 \|x_i\| \leq \|W\|_F^2 X_{\max},$$

$f(x_i; W, v) \rightarrow \infty$  enforces  $\|W\|_F^2 \rightarrow \infty$  as  $t \rightarrow \infty$ , thus  $\|W\|_2^2 \rightarrow \infty$  as well. This gets us

$$\limsup_{t \rightarrow \infty} \frac{\|W\|_F^2}{\|W\|_2^2} = 2.$$